NACA TM No. 1161

7857

NATIONAL ADVISORY COMMITTEE
FOR AERONAUTICS

TECHNICAL MEMORANDUM

No. 1161

WIND-TUNNEL TESTS ON VARIOUS TYPES OF DIVE BRAKES MOUNTED

IN PROXIMITY OF THE LEADING EDGE OF THE WING

By Bernardino Lattanzi and Erno Bellante

Translation of Relazione Tecnica No. 10: Ministero dell' Aeronautica
Direzione Superiore Studi ed Esperienze, I Divisione - Sezione
Aerodinamica, Guidonia, December 1942

NACA

Washington

May 1949

NATIONAL ADVISORY COMMITTEE FOR AERONAUTICS

TECHNICAL MEMORANDUM NO. 1161

WIND-TUNNEL TESTS ON VARIOUS TYPES OF DIVE BRAKES MOUNTED

IN PROXIMITY OF THE LEADING EDGE OF THE WING

By Bernardino Lattanzi and Erno Bellante*

SUMMARY

The present report is concerned with a series of tests on a model airplane fitted with four types of dive flaps of various shapes, positions, and incidence located near the leading edge of the wing (from 5 to 20 percent of the wing chord).

Tests were also made on a stub airfoil fitted with a ventral dive flap (located at 8 percent of the wing chord).

The hinge moments of the dive flaps were measured.

INTRODUCTION

Military necessities have forced almost every one of the belligerent nations to convert some of their high-altitude bombers into dive bombers. The greatest difficulty encountered in such a conversion program is the mounting of the dive brakes on the front spars of a completed airplane (and consequently near the leading edge of the wing) without spoiling the wing profile with slotted flaps protruding from the wing. Hence there arises the necessity of studying the behavior of the airplane mounting dive brakes on the front spar of the wing in the wind tunnel.

Sometimes design considerations make it necessary to mount the brake flaps on both the upper and the lower surface of the wing because the drag produced by the upper or the lower flaps alone is not sufficient and it is not possible to increase the lateral direction dimension as desired. The tests in the present report relate: (A) to a model airplane of 1:10 scale fitted with four dive brakes (two on upper, two on lower surface) located from 5 to 20 percent of the wing chord and (B) a 1:2-scale stub airfoil having a ventral brake flap located at 8 percent of the wing chord.

---

*"Prove Aerodinamiche su freni da picchiata posti in prossimita' del bordo d'entrata alare." Relazione Tecnica No. 10: Ministero dell' Aeronautica Direzione Superiore Studi ed Esperienze, I Divisione - Sezione Aerodinamica, Guidonia, December 1942.

A. WIND-TUNNEL TESTS ON AN AIRPLANE MODEL WITH VARIOUS TYPES OF

DIVE BRAKES MOUNTED NEAR THE LEADING EDGE OF THE WING

1. Dimensions and Construction of Airplane Model

The polished wooden model was equipped with movable wing and tail surfaces, the wing had a 1:3.42 taper ratio, with engine nacelle which originally was closed in front, and fitted with spinner, but which later was fitted with an engine without an operating propeller and air duct; it was constructed at 1:10 scale.

Its dimensions were as follows:

Wing span	L	$= 2.252$ m
Length	l	$= 1.760$ m
Mean chord	l_m	$= 0.2784$
Wing area	S	$= 0.6262$ m^2

The dive brakes, mounted at the upper and lower surface of each semispan, had the following dimensions and characteristics:

The model represented the high-speed CANT.Z 1018 bomber.

Brake flaps, type 1: from 8.5 to 8.24 percent of wing chord (flaps are trapezoidal); length 20.4 percent of semispan of wing; distance in percent between the leading edge and the median section of the brake flap: 4.9 percent of the wing chord in correspondence with the hinges situated in proximity of the engine nacelle axis (internal hinges); the same in correspondence to the external hinges: 6.2 percent; the angle of setting between the brake flaps open and the wing chord: 9 mm for each flap length (flap in position A); area of each flap: 0.575 dm^2 (fig. 1).

The tests with this type of flap revealed an aerodynamic phenomenon of great significance from the point of view of safety in flight and which was incorporated in the other three types of flaps having the following characteristics:

Brake flaps, type 2: from 7.64 to 8.24 percent of the wing chord; length: 19.53 percent of the semispan of wing; distance, in percent, between the longitudinal axis of the brake flap and the leading edge: 13.5 percent and 14.5 percent of the wing chord (respectively, corresponding to the external and internal hinges) in the case of 60° setting (angle between the tangent to the wing chord at the axes of rotation and flap); 16.2 percent and

17.6 percent of the wing chord at 90° setting; height of slot comprised between flap and wing profile: 8 mm in correspondence to the external hinge axis, 6 mm in correspondence to the hinge axis with flap open at 90° (flap in position B); flap area: 0.55 dm² (fig. 2).

Brake flaps, type 3: from 7.1 to 7.65 percent of wing chord; length: 19.53 percent of semispan of wing; distance, in percent, between longitudinal axis of brake flap and leading edge: 17.1 percent and 17.9 percent of wing chord in the case of 60° setting; 20 percent and 20.6 percent at 90° setting; height of slot between flap and wing profile: 10 mm in correspondence to the external hinge axis, 8 mm in correspondence to the internal hinge axis for flap inclined at 90° (flap in position C); flap area: 0.506 dm² (fig. 3).

Brake flaps, type 4: from 10.65 to 11.15 percent of wing chord; length: 20.4 percent of semispan of wing; distance between longitudinal axis of brake flap and leading edge: 16.4 percent and 17.6 percent of the wing chord at 60° setting; 20.9 percent and 21.5 percent at 90° setting; height of slot between flaps and wing profile: 10 mm in correspondence to the external hinge axis, 8 mm in correspondence to the internal hinge axis with flap inclined at 90° (flap in position D), (figure 4).

Each flap had four slots of 39.2 × 4 mm and two of 108 × 4 mm. The area of each flap (solid area only): 0.62 × 4 dm²; total area of each flap: 0.77 dm²; percentage of air space with respect to total flap: 12.4 percent.

During the tests, the flaps of type 2 were located in position C (16.8 percent and 18.2 percent for 60° setting; 19.8 percent and 20.6 percent at 90°) and those of type 3 in position B (13.5 percent and 14.9 percent for 60° setting and 16.8 percent and 17.9 percent for 90° setting.

2. Test Procedure

The tests were run in the 3-meter tunnel No. 5 with double return passage by means of six-component balances at 60 m/s airspeed, corresponding to an effective Reynolds number of 1,610,000, with the exception of a check test at 100 m/s (R = 2,370,000), in stages of 3° each at first, up to maximum lift, and after that by degrees at incidences from -6° to 5° for better recording of a phenomenon which will be described later. The brake flaps of types 2 and 3 besides being tested in relative positions B and C were also tested in positions C and B, respectively.

The tests were run with stabilizer set at -1° 16' and elevator at 0° with respect to stabilizer.

The wall corrections are reproduced for the tests near -6° at $C_{p_{max}}$ but disregarded in the others, since they were very nearly equal to zero. The moments are always referred to the leading edge of the CMA. (It should be noted that the nondimensional coefficients used are in the Italian form

$$C_r = \frac{R}{\rho s v^2}, \quad C_p = \frac{P}{\rho s v^2}, \quad C_m = \frac{M}{\rho s v^2 l}$$

which are equal to in NACA notation

$$C_r = \frac{1}{2}C_D; \quad C_p = \frac{1}{2}C_L, \quad C_m = \frac{1}{2}C_M \Big)$$

3. Test Results

The model, mounted with dive brakes closed and with flaps set at 0°, showed a 100 $C_{r_{min}}$ of 0.86, which is perhaps a little low with respect to the real value, because of the primitive construction of the model with completely closed engine nacelles, and the perfect polish of the model itself, factors which are not negligible at Reynolds numbers as high as those used in the test. The maximum lift coefficient C_p was 0.585, the maximum efficiency 19.65 (fig. 5). The test on the same model with dive flaps fitted with cowlings and air ducts and electric motor, but without propellers, yielded a 100 $C_{r_{min}}$ of 1.1.

The opening of the brake flaps of type 1 produces an irregular variation of the lift curve (fig. 6), which is reflected in the moment curve C_m and jeopardizes the stability of the aircraft in a very critical stage of flight (fig. 24).

The angle of $C_{p_{min}}$ rises from 13° 30' to beyond 20°; its exact value was not determined; the value of 100 $C_{r_{min}}$ increases to 5.5.

Simultaneous opening of brakes and flaps improved the lift curve C_p (fig. 7) so as to remove the difficulty at a 60° flap angle (fig. 8).

The hope of eliminating the phenomenon without making use of the flaps prompted a series of tests at the angles of incidence at which the phenomenon appeared, by varying the dimensions of the slot between the edge of the flaps and the wing profile, as well as by closing successively the top and bottom brakes, with the original and larger slots.

The results are reproduced in figure 9: When successively increasing each dorsal slot by 2, 4, and 6 mm, the phenomenon, while tending to diminish, still subsists (curves a, b, c, and d) but it disappears upon

closing the dorsal brakes while leaving the ventral brakes unaltered (curve e) and, also, by closing only the ventral brakes. In this, as in the preceding case, the width of the slot is of negligible importance (slots increased 4 and 6 mm, curves f and g). Therefore, the phenomenon subsists only when either the ventral or dorsal face disturbs the wing surface, whatever the slot width (within practical limits) between brake flaps and wing surface.

With the object of eliminating the difficulty, a proposal was made to adopt one of the two types of flaps 2 and 3 for testing in positions B and C.

Figures 10, 11, and 12 represent the comparison of the lift, drag, and moment curves C_p, C_r, and C_m corresponding to the brake flaps of type 2, in positions B and C (curves a and b) and of brake flap, type 3, in positions C and B (curves c and d), always at $\alpha = 90°$ setting. The values of C_p are negative and approximately constant noting the considerable oscillations registered on the balance) between -4° and 2°; the best solution of the four examined proved to be that of brake flap type 2 in position C.

Figures 13, 14, and 15 show the contrast between the lift, drag, and moment curves C_p, C_r, and C_m corresponding to these conditions, but with brake flaps set at 60° (brake flaps, type 2, in positions B and C, curves a and b; brake flaps, type 3, in positions C and B, curves c and d). The values of C_p have a more sinuous variation in the same interval and assume positive values. The resultant greater instability is therefore attributable solely to the incidence of the flaps with respect to the wind, provided that the effect due to a variation in slot height which in this case ($\alpha = 60°$) is negligible with respect to the other.

The condition of the type 2 flaps, position B ($\alpha = 60°$), was also tested throughout the range of -6° to 5° at 100 m/s airspeed in order to verify that the higher speed did not introduce some new phenomenon (curve e). The slight divergences in the more critical distance are, moreover, imputable to the difficulty in reading the balances at such speeds.

A very noteworthy improvement is having a little air reach the part of the wing situated aft of the brake flaps. The flaps of type 3 were perforated as shown in figure 3 A, by means of two rows of holes gradually decreasing in diameter from 5 to 3 mm, with the axis inclined at 20° to the horizontal passing through the upper eye of the flap. The full (or solid) area is 0.4566 dm^2; the percentage of air space with respect to the flap area is 9.76 percent.

In figures 16, 17, and 18, the curves for C_p, C_r, and C_m are shown for the perforated flaps, type 3, situated in position C at angles of 60°,

90°, and 110° (curves a, b, and c) and in position B at angles of 60°, 90°, and 110° (curves a, b, and c) and in position B at angle of 90° (curve d). An irregular variation is again noted around zero lift on the flaps at 60° (position C); it ceases as the angle increases. The best condition (curve c) is referred to the angle of 110°; in this case, the value 100 $C_{r_{min}}$ = 4.4 is obtained, which is, however, a little low.

For the airplane in question, it was, therefore, more suitable to use the perforated flaps of type 3 in position C, at 90° angle, represented in figures 19 and 20, where the curves of C_p, C_r, and C_m are shown plotted for the range of -6° to 22° incidence. From it follows a $C_{r_{min}}$ value of 4.74 for an angle of around 0° and a $C_{p_{min}}$ value of about 47 at 21°, obtained after a drop in lift at an incidence of 16° 30' (100 C_p = 43).

With the object of obtaining a more efficient braking action, a test was therefore made on brake flap, type 4, which was larger than the others, as already indicated. Figures 21, 22, and 23 represent its lift, drag, and moment curves for two positions of opening, 60° and 90° (curves a and b). The irregular variation near zero lift is still evident at 60°, but has almost disappeared entirely at 90° angle. The maximum lift which follows at about 0.51 for the two brake settings has a smaller gradient than the perforated flap of type 3. The 100 $C_{r_{min}}$ is 5.13 and 5.7, respectively.

The subsequent table gives the values of the moment gradient referred to the lift $\dfrac{dC_m}{dC_p}$, corresponding to 100 C_p = 25 and the ratios

$$\frac{100 \; \Delta C_r}{\text{total area of flaps}}$$

and

$$\frac{100 \; \Delta C_r}{\text{solid area of flaps}}$$

for the principal conditions of the test.

Conditions	$\dfrac{dC_m}{dC_p}$	$100\,C_{r_{min}}$	$100\,\Delta C_r$	Area of 4 flaps, dm^2	$\dfrac{100\,\Delta C_r}{\text{Area of 4 flaps}}$	$\dfrac{100\,\Delta C_r}{\text{Solid area of flaps}}$
Brake flaps and slots closed	0.382	0.86				
Type 1, brake flaps open — slots closed	0.52	5.5	4.64	2.3	2.01	2.01
Type 1, brake flaps open — slots at 30°	0.414	5.8	4.94	2.3	2.15	2.15
Type 1, brake flaps open — slots at 60°	0.424	6.5	5.64	2.3	2.45	2.45
Type 3, perforations, slots 90°, position C	0.46	·4.74	3.88	(2) 2.025 1.83	1.92	2.12
Type 4, slots open 60°	0.520	5.13	(1) 4.03	(2) 3.08 2.48	1.31	1.63
Type 4, slots open 90°	0.520	5.58	(1) 4.48	(2) 3.08 2.48	1.45	1.81

(1) This ΔC_r was computed for the $100\,C_{r_{min}} = 1.1$ (engine with cowling with air passage).

(2) The higher values refer to the total area of the flaps.

Figure 24, which contains the C_m coefficients in functions of C_p, further shows, besides the curves corresponding to type 3 brake flaps (curve a), those of the airplane with brake flap closed and slots open (curve b), type 1 brake flaps open (position A) and slots closed (curve c); type 1 brake flaps open, slots at 30° and 60° (curves d, e); and type 4 brake flaps open at 60° and 90° (curves f and g).

Naturally, these values are subject to modification in the case of the real airplane, as the model had been tested without functioning of the propellers.

With the object of determining the value of the nondimensional coefficients C_μ of the hinge moments, a test was made on a wing root or stub of 1:5 scale, fitted with end plates, set at 3° incidence, at 60 m/s airspeed in tunnel No. 2 of 2 m (effective Reynolds number of 2,800,000) by bolting a steel bar midway of each flap after removing the support straps and applying a load at the other end to balance the brake in the various positions of opening. The load was applied on a scale pan located outside of the test chamber and connected by means of a very fine wire to the end of the bar.

The test was made on the type 3 brake flaps without holes, in position C, and on type 4. The results shown in figures 25 and 26 have been referred to the value of the mean chord λ ($\lambda = 0.046$) of the brake flap and its area s (0.02025 m²). It will be noted that the curves, not much different for both the upper-and lower-surface flaps, show a maximum value of $C_\mu = 0.7$ at the $\varphi = 20°$ opening and an average value of $C_\mu = 0.55$ at openings $\varphi = 30°$ to 90° (type 3 flaps, fig. 25); a C_μ value increasing to 0.45 from 0° to 35° and an average of $C_\mu = 0.45$ up to $\varphi = 90°$.

B. AERODYNAMIC TESTS ON A MODEL STUB WING WITH VENTRAL BRAKE FLAP

Dimensions and Construction

The 1:2-scale model was tested at 40 m/2 airspeed. Its general characteristics (fig. 27) were as follows:

Span	L	= 1.802 m
Chord	l_m	= 0.930 m
Area	S	= 1.675 m²

The brake flap, mounted on the upper surface with the hinges corresponding to 8 percent of the wing chord, had the following characteristics: height - 94 mm; length - 1802 mm; depth of slot - 16 mm; inclination of open slot to profile chord - 67°; 10 horizontal slots of 97 × 18 mm; clearance between axes - 177 mm.

Test Procedure

The tests were run at 40 m/s airspeed, but, in view of the great chord length, at an effective Reynolds number of 3,470,000.

The tests, ranging from -18° to 6°, covered the following conditions:

(a) Wing with brake flap closed C_r, C_p, C_m

(b) Wing with brake flap open and slots closed C_p, C_r, C_m

(c) Wing with brake flap open and slots open C_p, C_r, C_m

(d) Hinge moments of brake flap at maximum opening with slots closed

(e) Hinge moments of brake flap at maximum opening with slots open

(f) Qualitative measurement of wake turbulence with brake flap closed

(g) Qualitative measurement of wake turbulence with brake flap open and slots open and closed

The geometric aspect ratio of 1.94 was increased by the addition of two elliptical end disks of 1540 × 710 mm dimensions (15-mm thickness). The virtual aspect ratio is equal to about 3.35.

Results

Figure 28 shows the three C_r curves for conditions a, b, and c, freed from end disk drag and streamline wires; figure 29, the three lift curves (conditions a, b, and c); and figure 30, the three moment curves C_m.

The calibration for determining the parasite drag of the end disks was effected by suspending one of the two disks secured to two pairs of steel wire arranged in vee shape and measuring the divergence of the system from the vertical under the action of the wind by means of a telescope.

As a check on the accuracy of measurement, the wing, complete with disks, was suspended again by the same method under conditions 1; it proved in perfect agreement with the data obtained previously.

The results are shown in the following table:

Conditions	$100\ C_{r_{min}}$	$\alpha C_{r_{min}}$	$100\ C_r$ $(\alpha = -6^o)$	$\alpha C_p = 0$	$\alpha C_m = 0$
a	0.36	$\sim -1^o$	0.73	$-1^o\ 25'$	$-3^o\ 10'$
b	5.06	$\sim\ 6^o\ 10'$	7.22	$-18^o\ 36'$	$-16^o\ 40'$
c	5.01	$\sim\ 5^o\ 40'$	6.86	$-17^o\ 12'$	$-16^o\ 33'$

The hinge moments were measured after bolting a steel plate to the middle of the flap after removing the support straps and applying a load at the other end so as to balance the brake in the position of maximum opening.

Figure 31 gives the nondimensional hinge-moment coefficients C_μ for the conditions b and c.

The qualitative measurements of the wake turbulence were made with wood tufts, with brake flap closed (condition a) and brake flap open and slots half open and half closed (conditions b and c).

The results are visible in the appended photographs. The open flap, whether with slots open or closed, tows behind it an extremely turbulent wake as far as the trailing edge.

With the introduction of the brake flap, the minimum drag becomes about 14 times higher, but the angle for zero lift passes from $-1^o\ 25'$ to $-17^o\ 12'$ and $-18^o\ 36'$, respectively, for the flaps with slots open and closed, which renders the application of the above-mentioned flap impossible for flight in vertical dive, since the tailplane is rendered more nonlifting in the case of obstinate centering difficulty.

The gradient of the moment referred to the lift $\left(\dfrac{dC_m}{dC_p}\right)$, which in the case of the wing without brake flap amounts to 0.233 is not exactly definable in the case of the wing with brake flap, because of the tortuous shape of the two curves b and c, but can be said to average the above value.

The hinge moments in condition 2 exceed those in condition 3 by about 8 percent.

CONCLUSIONS

The experiments performed on an airplane model fitted with dorsal and ventral brake flaps on each semispan, near to the leading edge of the wing (5 to 20 percent of wing chord) show an irregular variation of the lift curve which, as reflected in the longitudinal moment curve, endangers the stability of the airplane. This drawback was removed by the use of perforated flaps.

It was found more convenient from the aerodynamic point of view to use both holes and slots, as the ratio $100 \Delta C_r$ to full (or solid) area of flaps, shifting for the case in point from 2.12 to 1.81, presents an increment of 17 percent.

It was therefore found impossible to utilize brake flaps without openings, as it may result in a worsening of the wing characteristics, since the opening is in a zone in which the boundary layer is laminar.

The experiments on the stub wing fitted with ventral brake flap (located 8 percent of wing chord) indicate that the zero lift angle is displaced from $-1^\circ 25'$ to $-17^\circ 12^\circ$ and $-18^\circ 36'$ for brake flaps with slots open or closed, which implies a strong negative lift in a vertical dive, if not persistent difficulty of balancing.

Translated by J. Vanier
National Advisory Committee
for Aeronautics

Scale 1:4 of model

A   B

80

Axis of rotation

30   30

27   23

230

Hinge axis   Hinge axis

A   B

Engine axis

Position A

Scale 1:2 of model

15

3   9   Section AA

9

9

17

3   Section BB

9   3

9
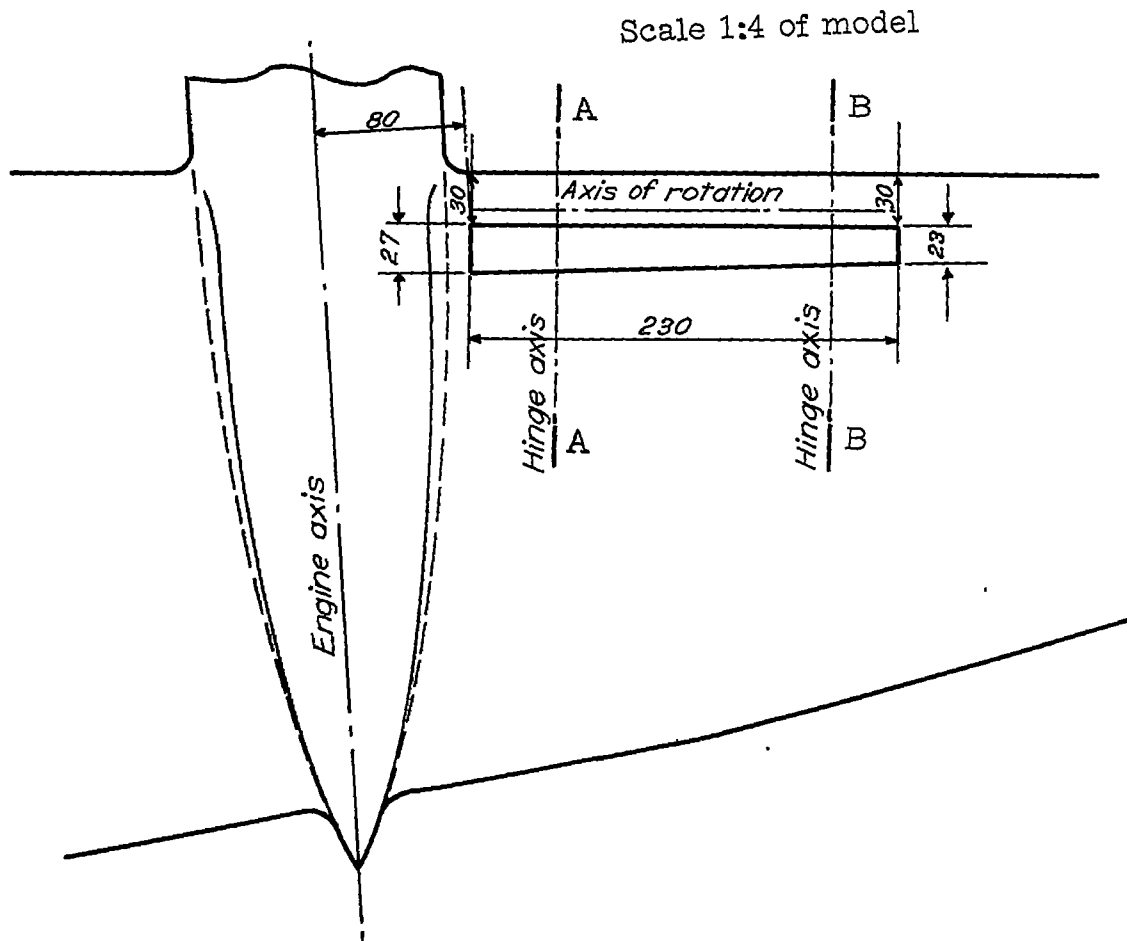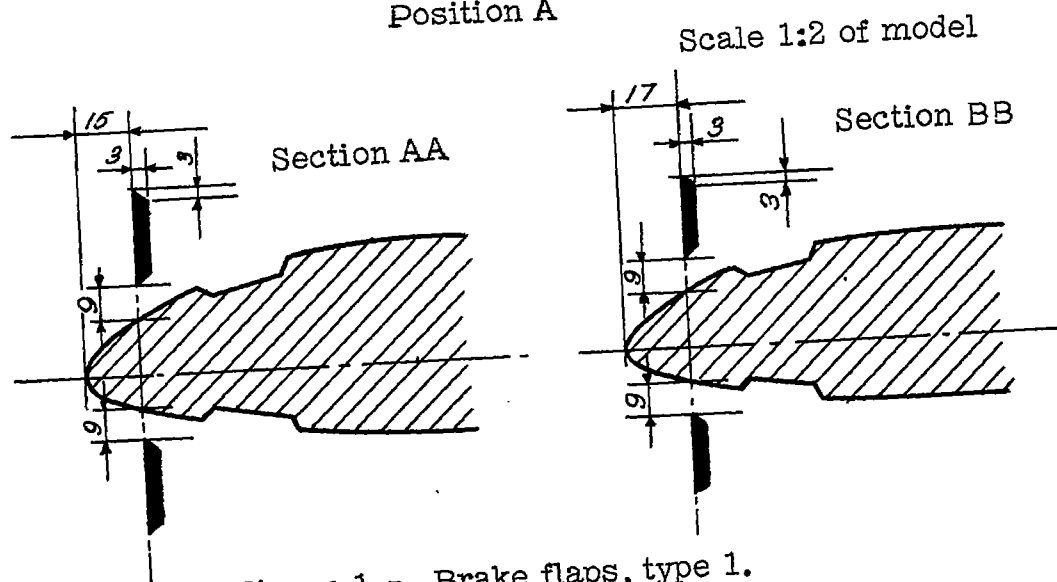
Figure 1.-   Brake flaps, type 1.

Scale 1:4 of model

Figure 2.-   Brake flaps, type 2.

Scale 1:4 of model
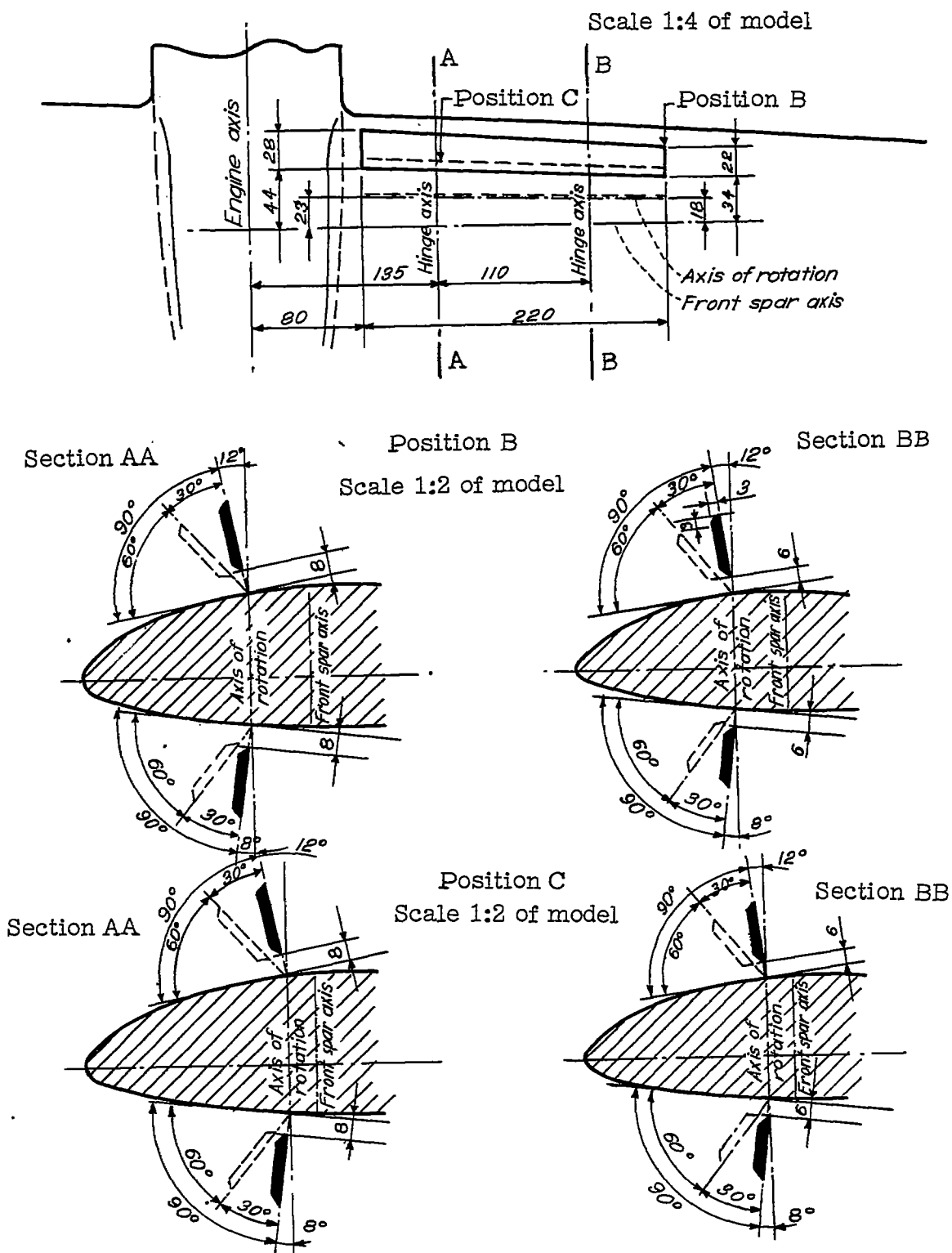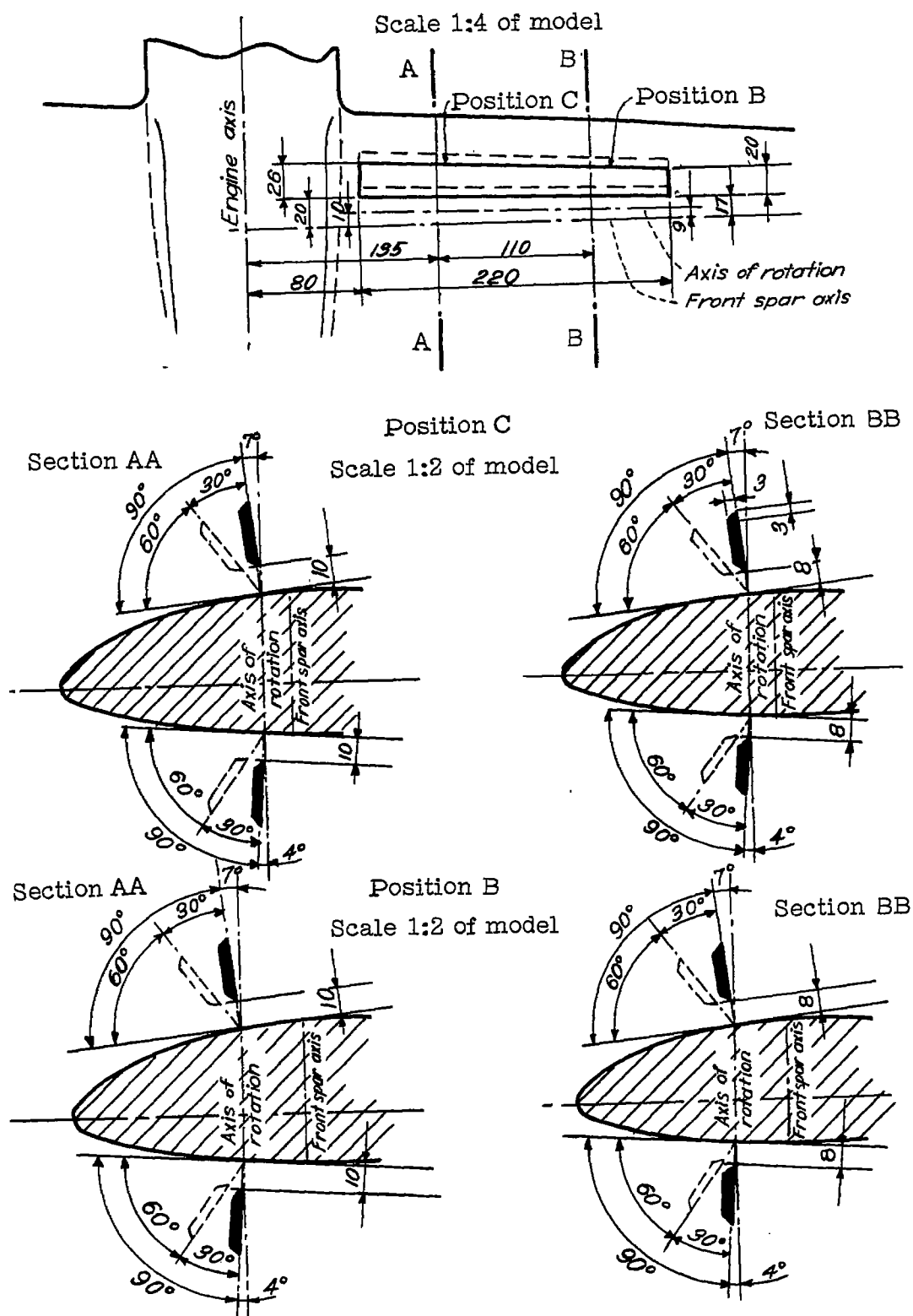
Figure 3.-   Brake flaps, type 3.

Position C
Scale 1:2 of model

Section AA

Section BB

30° 20°
7°
60°
10

30° 20°
7°
60°
8

Axis of rotation

Front spar axis

Axis of rotation

Front spar axis

60°
30° 20°
4°
10

60°
30° 20°
4°
8

Section AA

Position B

Section BB

7°
90°
10

7°
90°
8

Axis of rotation

Front spar axis

Axis of rotation

Front spar axis

90°
4°
10

90°
4°
8

Plane of brake flap

220
45.5 11 98 11 45.5 4.5

20°

6.5 4.5

26

19

6.5

20

Figure 3a.— Brake flaps, type 3 - perforations.

Scale 1:4 of model

Position D

Scale 1:2 of model

Section AA

Section BB

Figure 4.-   Brake flaps, type 4.
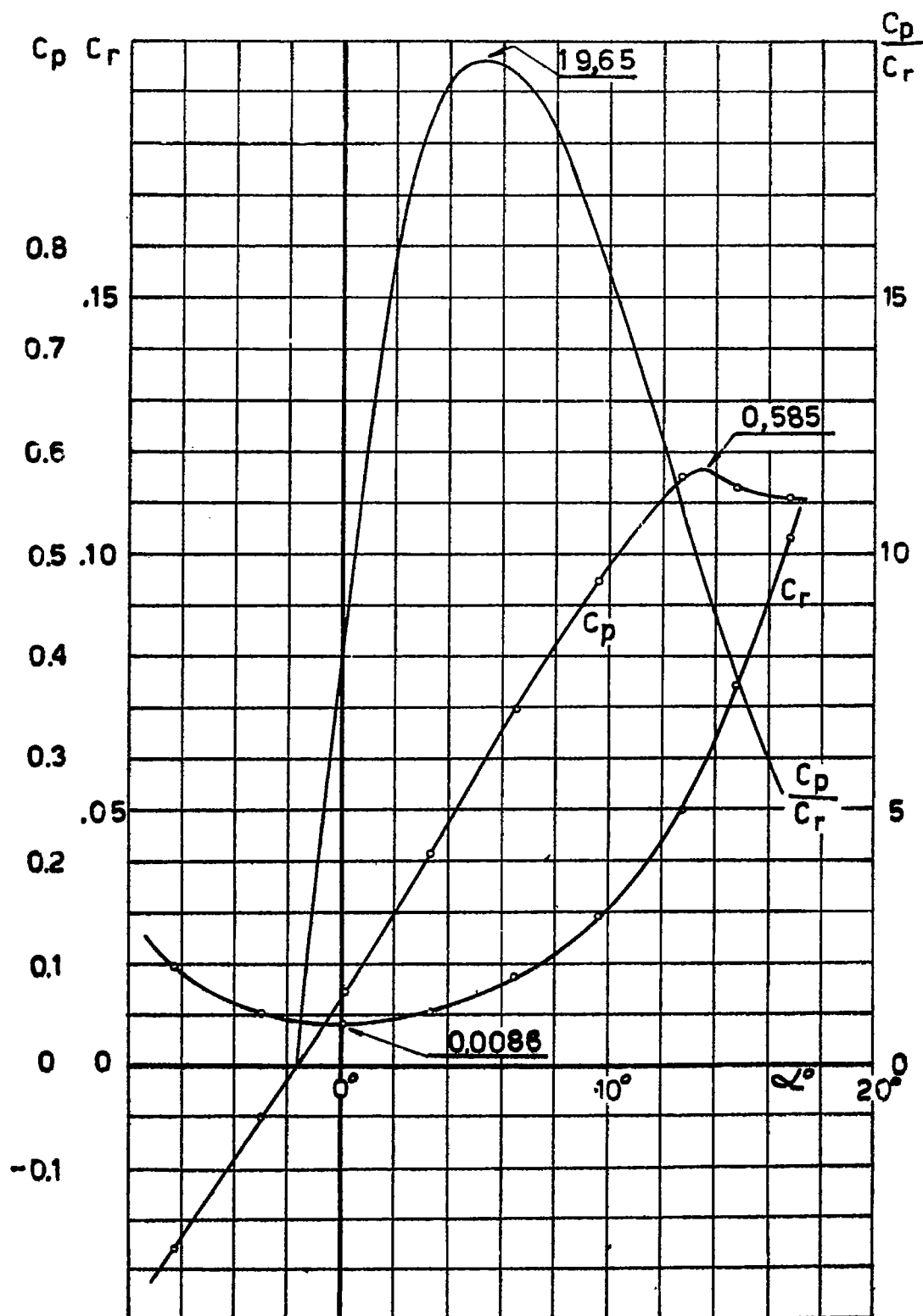
Figure 5.- Without brakes.
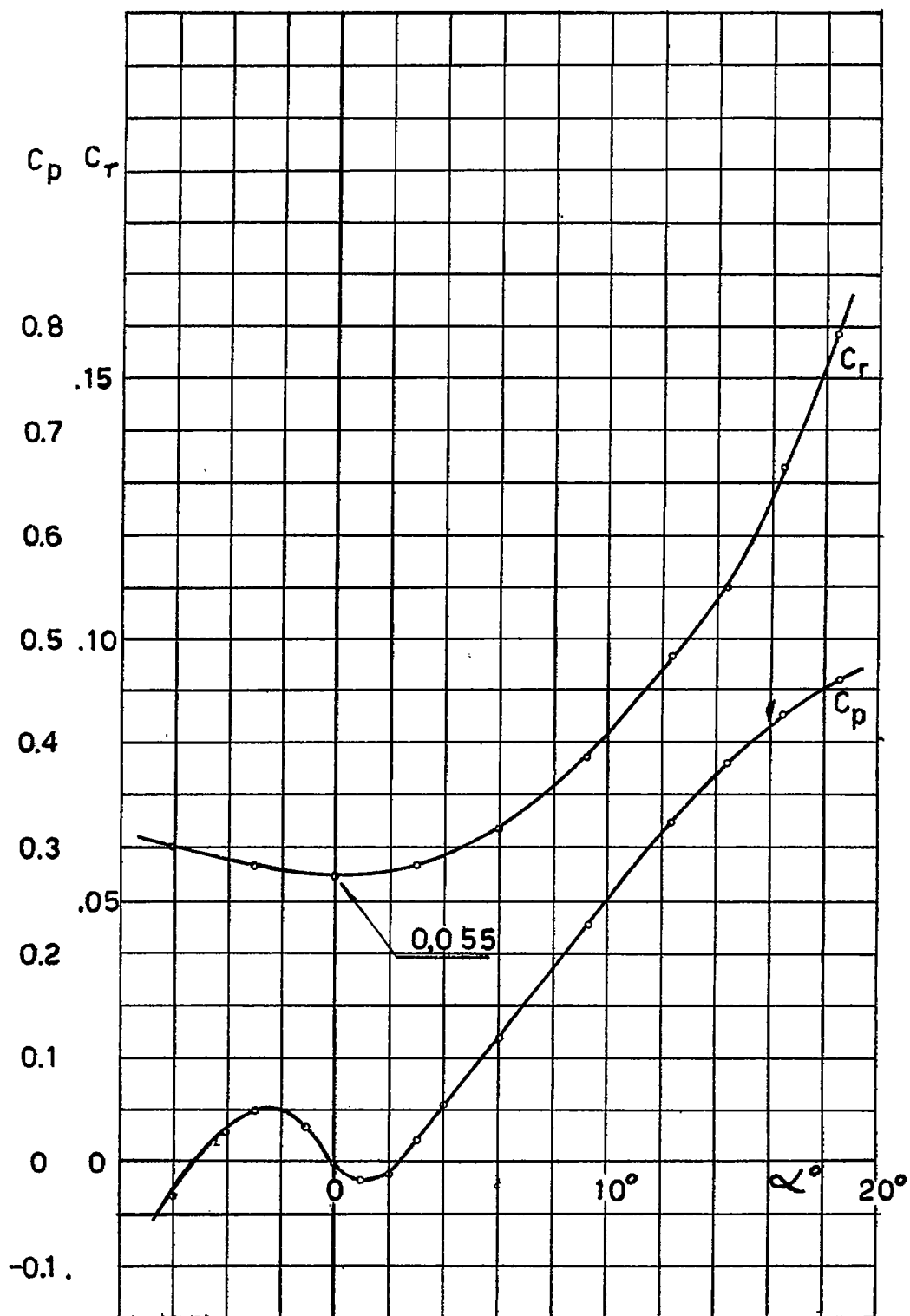
Figure 6.-   Brake flaps, type 1 - 90⁰ open.
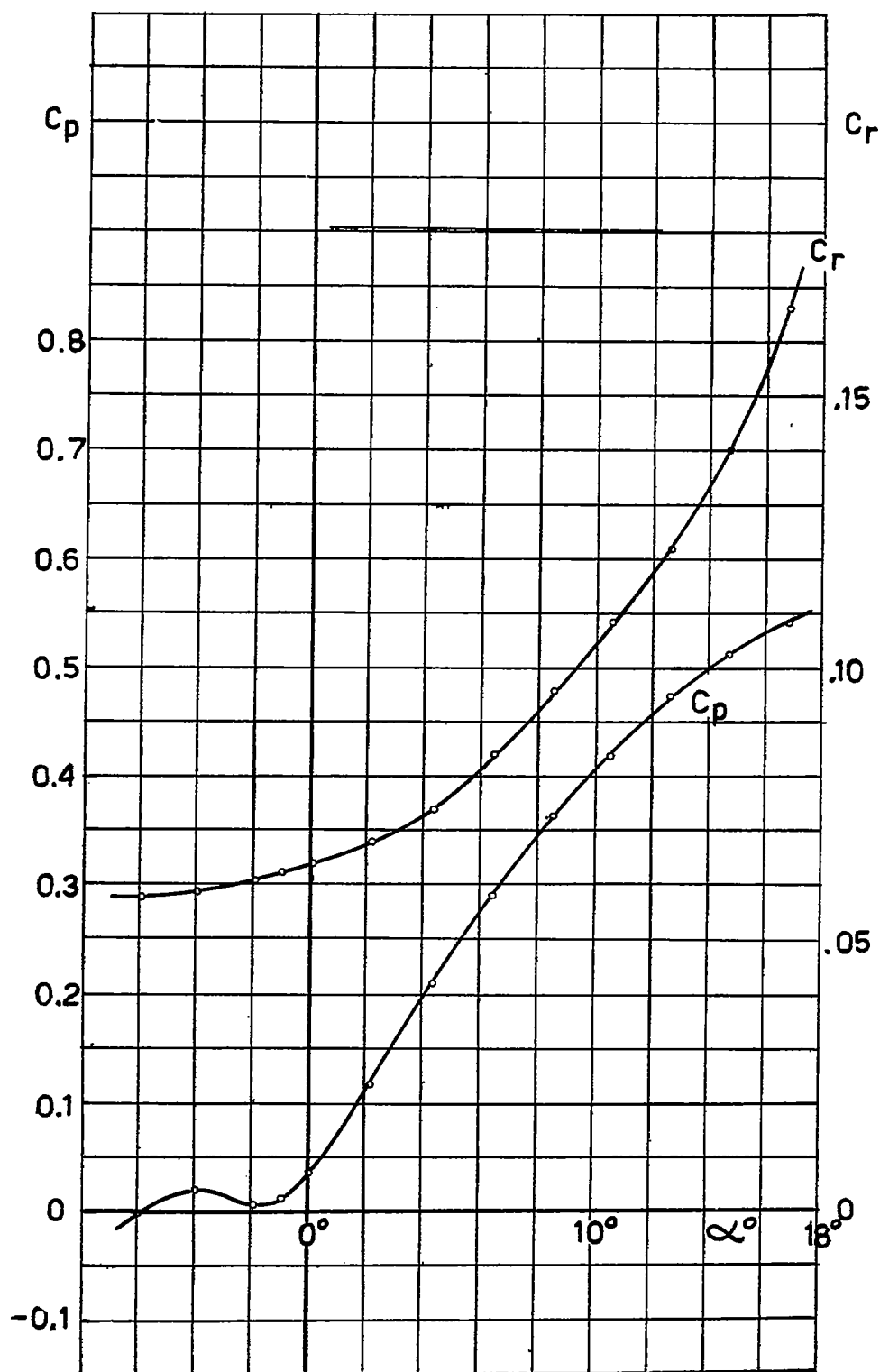
Figure 7.-   Brake flaps, type 1 - 90° open - flap 30° open.
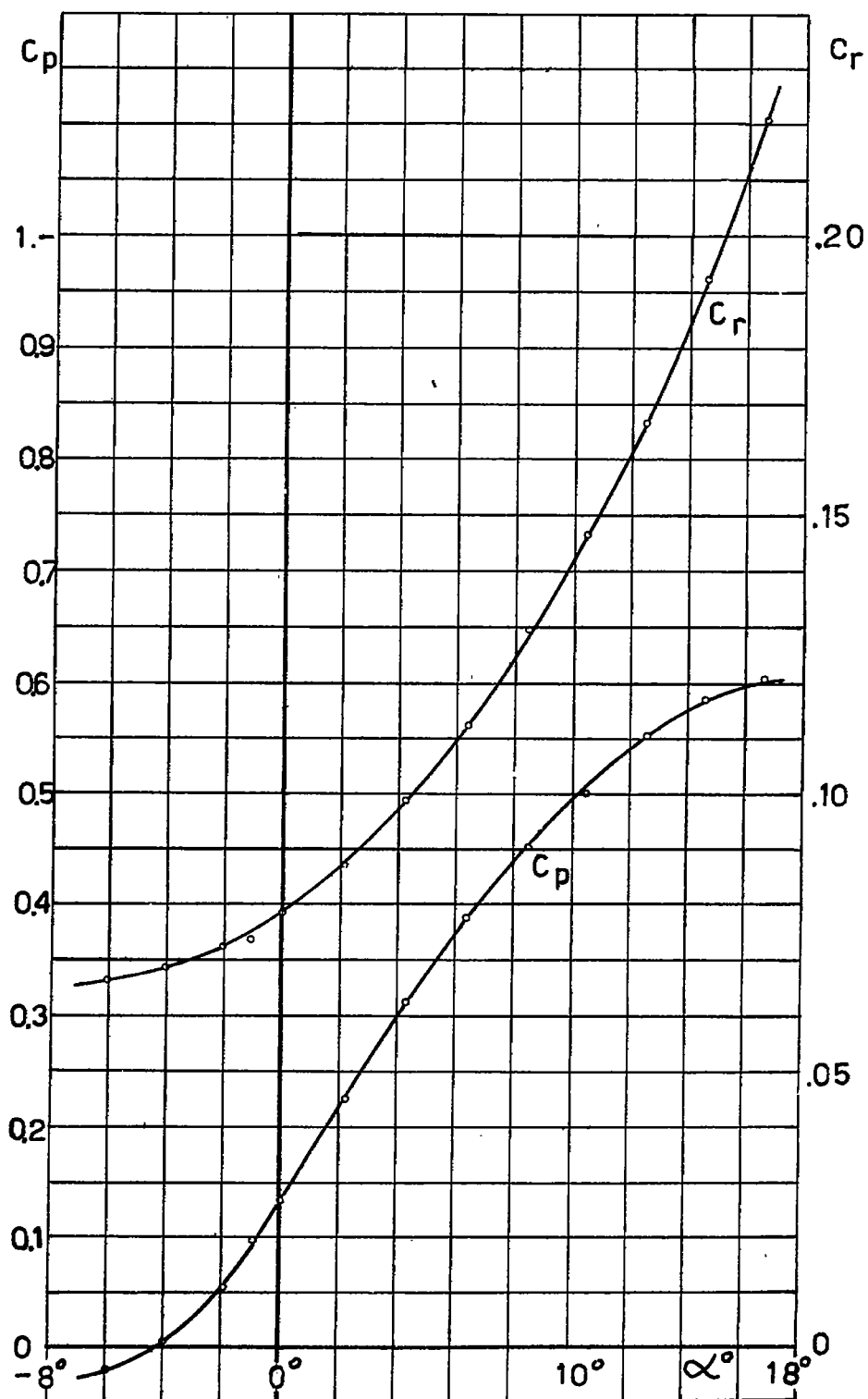
Figure 8.- Brake flaps, type 1 - 90° open - flap 60° open.

Solution	Upper Surface		Lower Surface	
	Angle of opening	Slot m/m	Angle of opening	Slot m/m
a	90°	9	90°	9
b	"	11	"	"
c	"	13	"	"
d	"	15	"	"
e	0°	—	"	"
f	90°	13	0°	—
g	"	15	0°	—
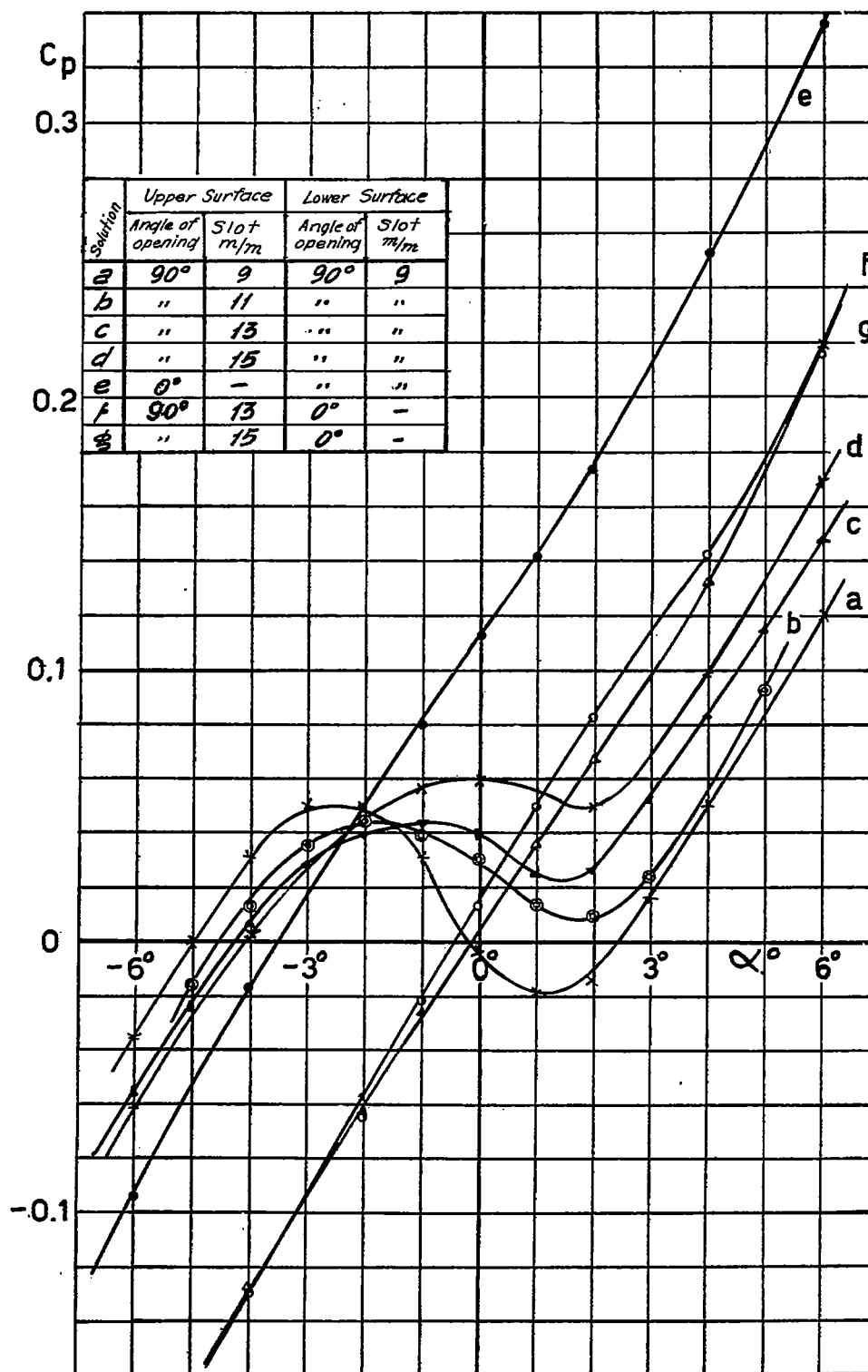
Figure 9.- Brake flaps, type 1.
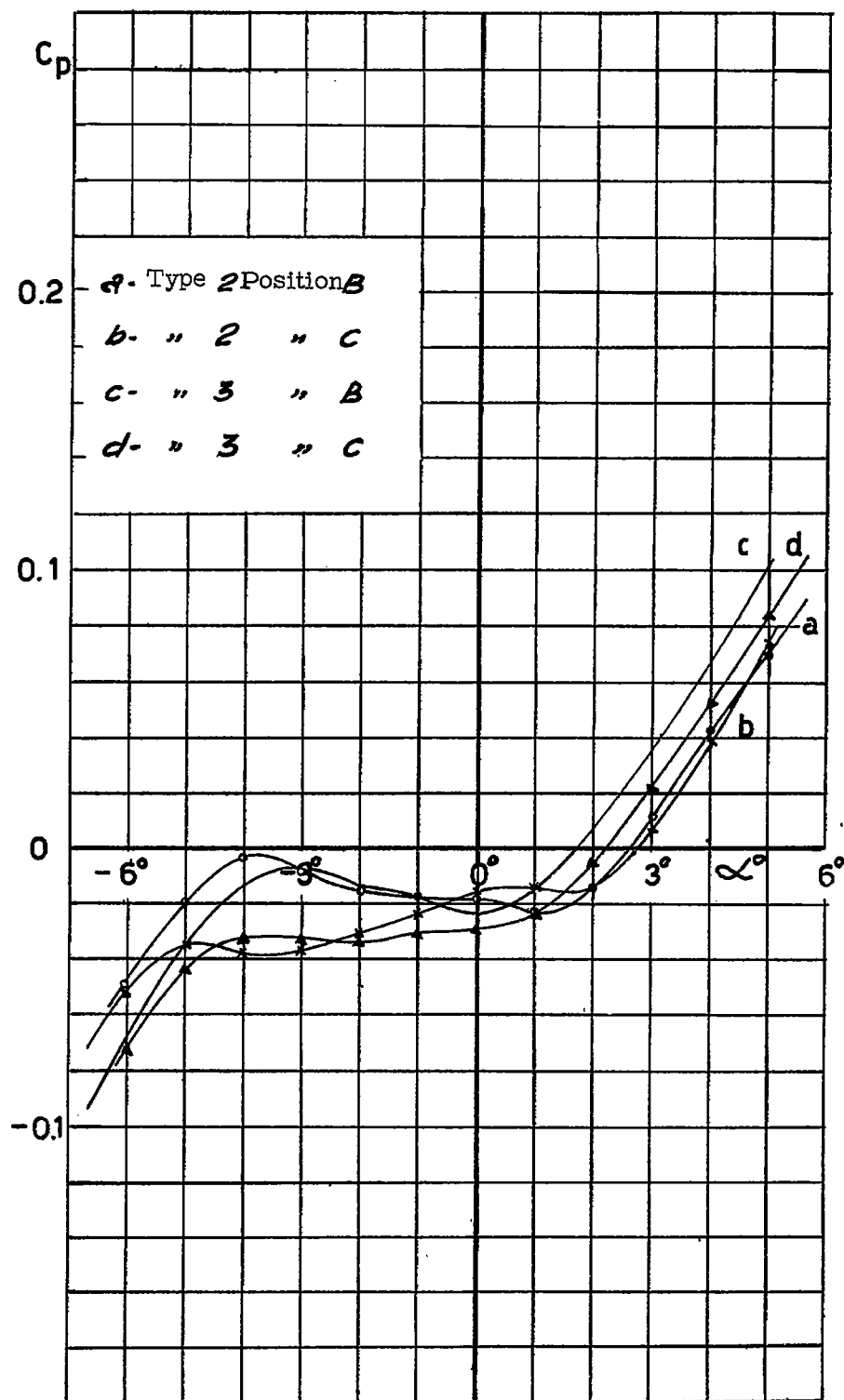
Figure 10.-   Brake flaps, types 2 and 3 - 90° open - lift.
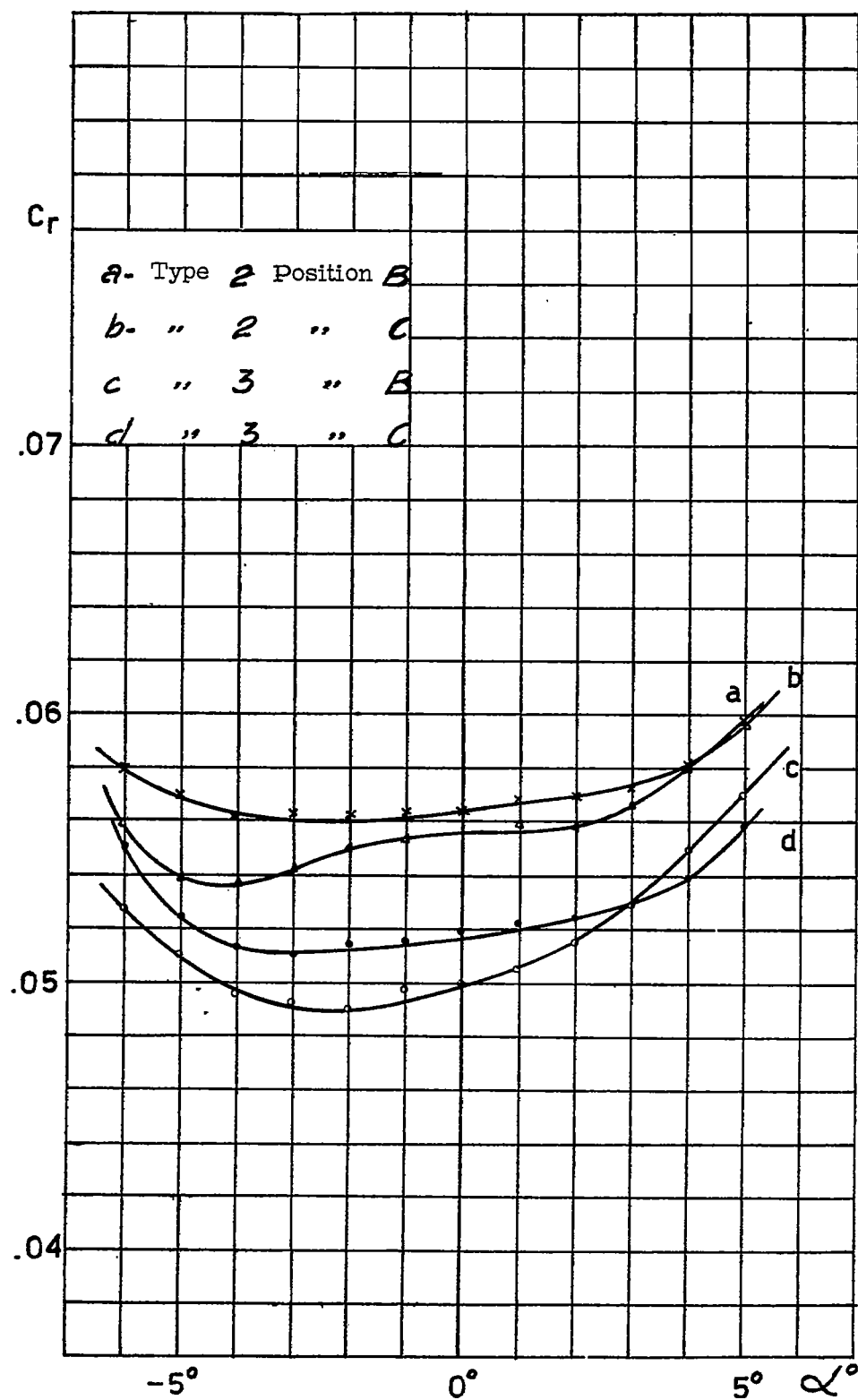
Figure 11.-   Brake flaps, types 2 and 3 - 90° open - drag.
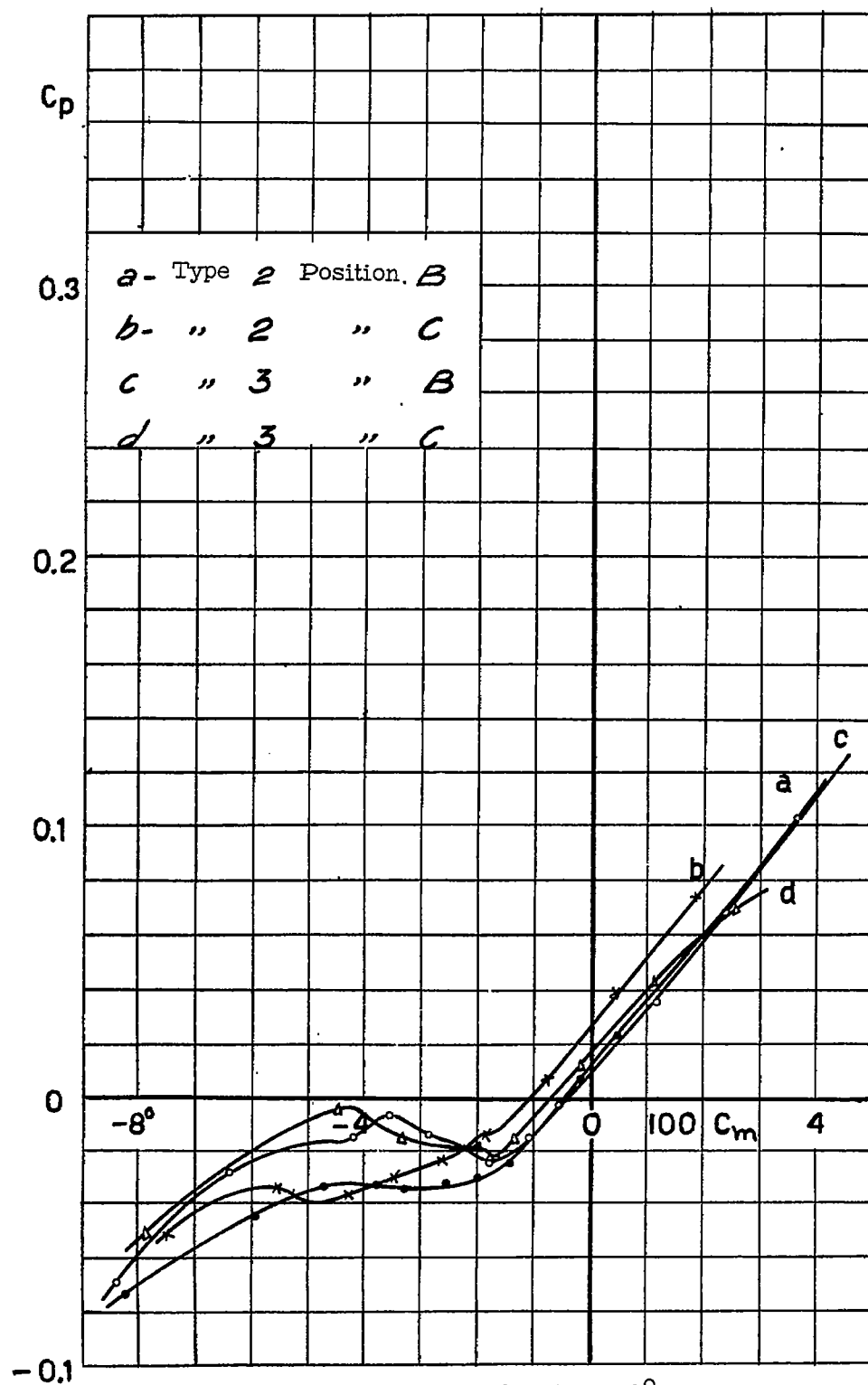
Figure 12.-   Brake flaps, types 2 and 3 - 90° open - moments.
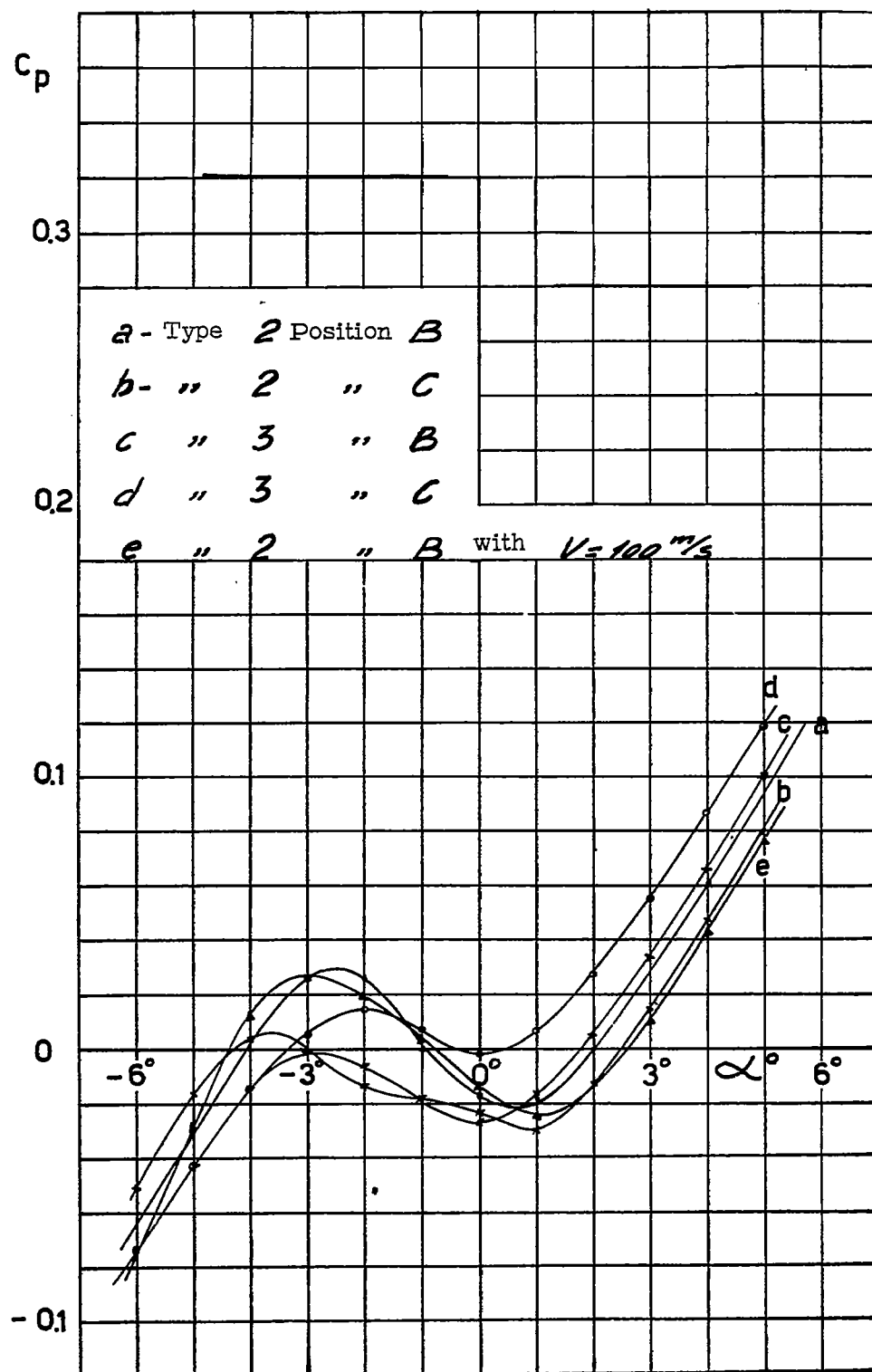
Figure 13.-   Brake flaps, types 1 and 2 - 60° open - lift.
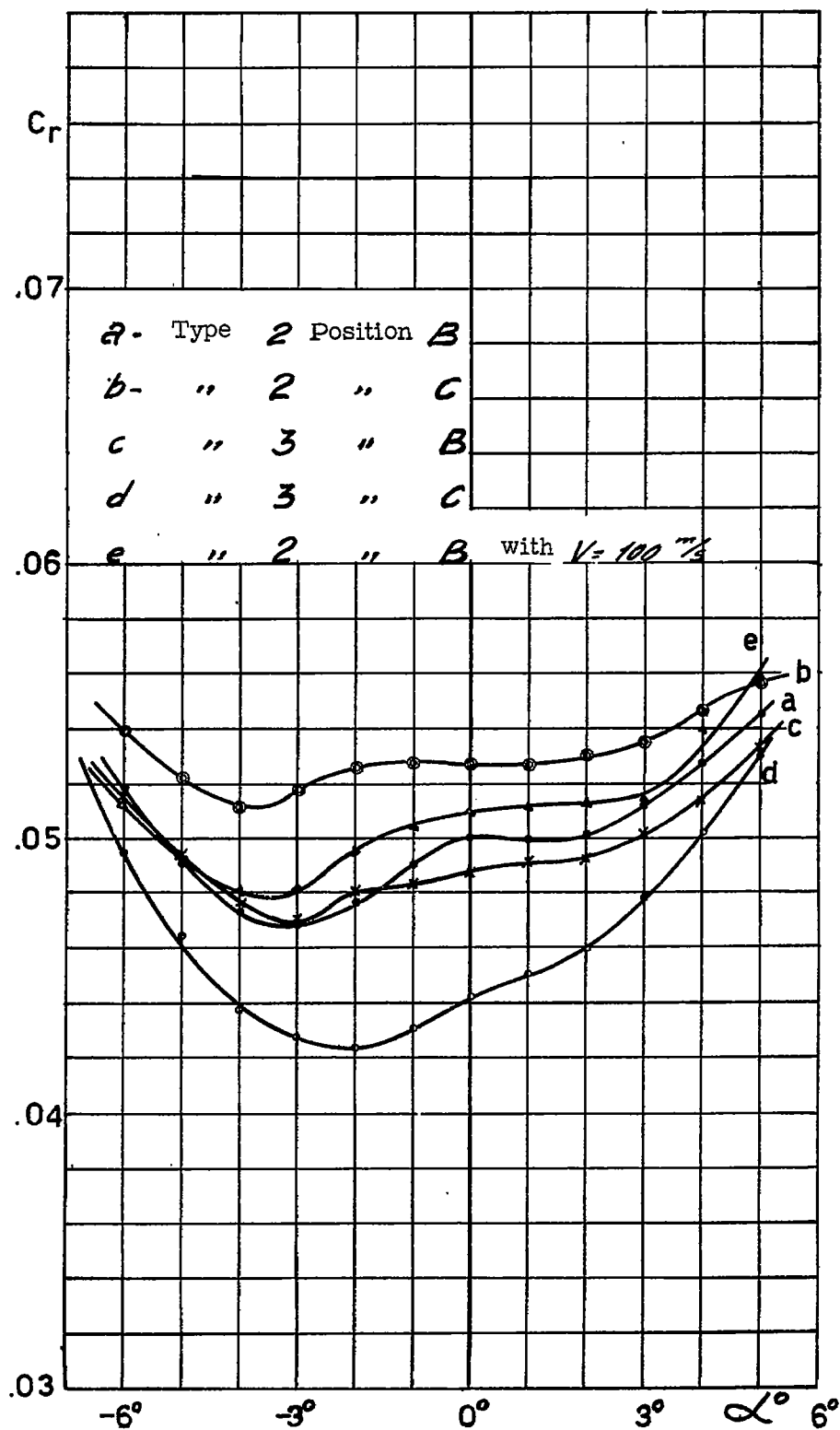
Figure 14.-   Brake flaps, types 2 and 3 - 60° open - drag.
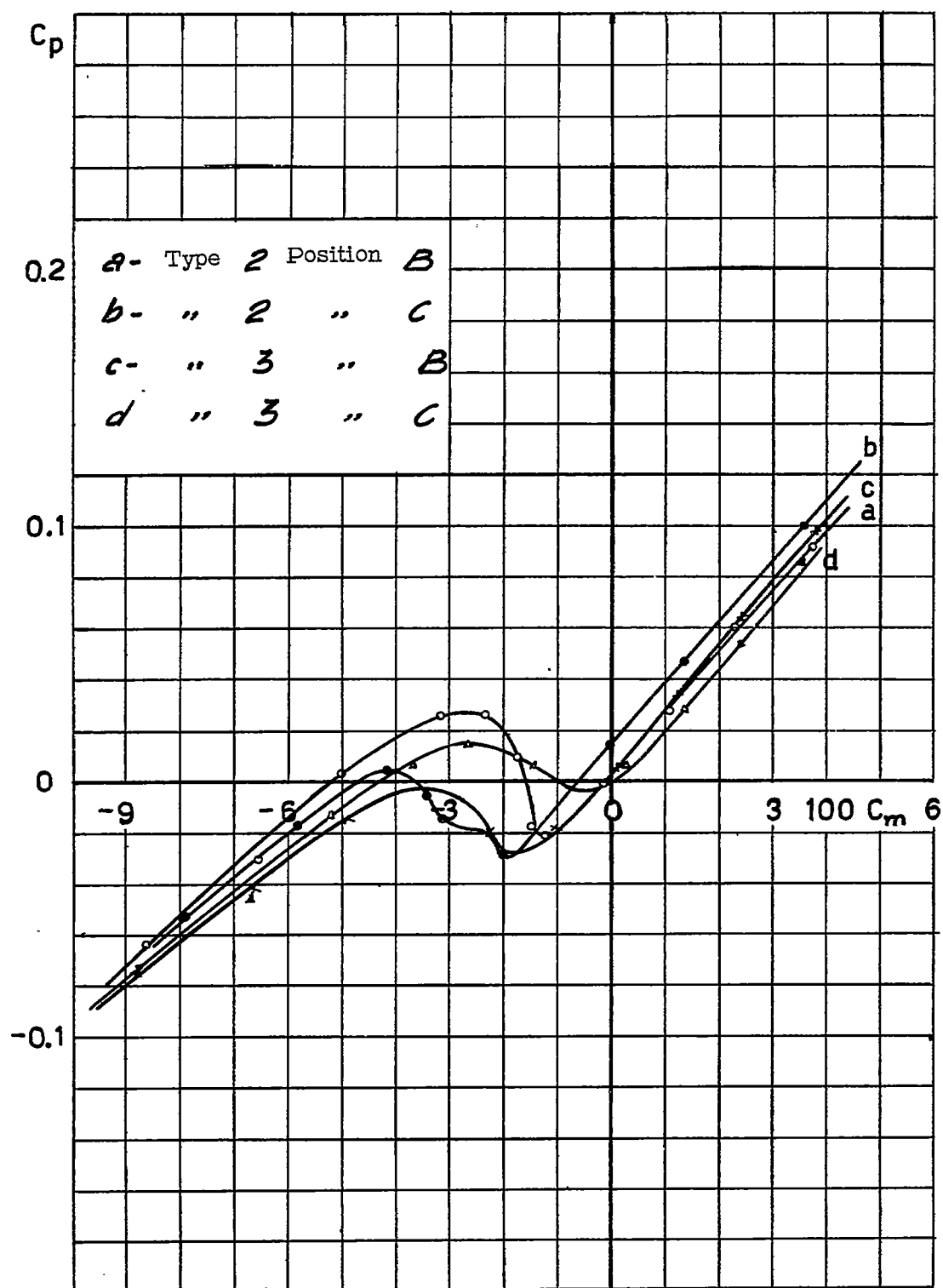
Figure 15.-   Brake flaps, types 2 and 3 - 60° open - moments.
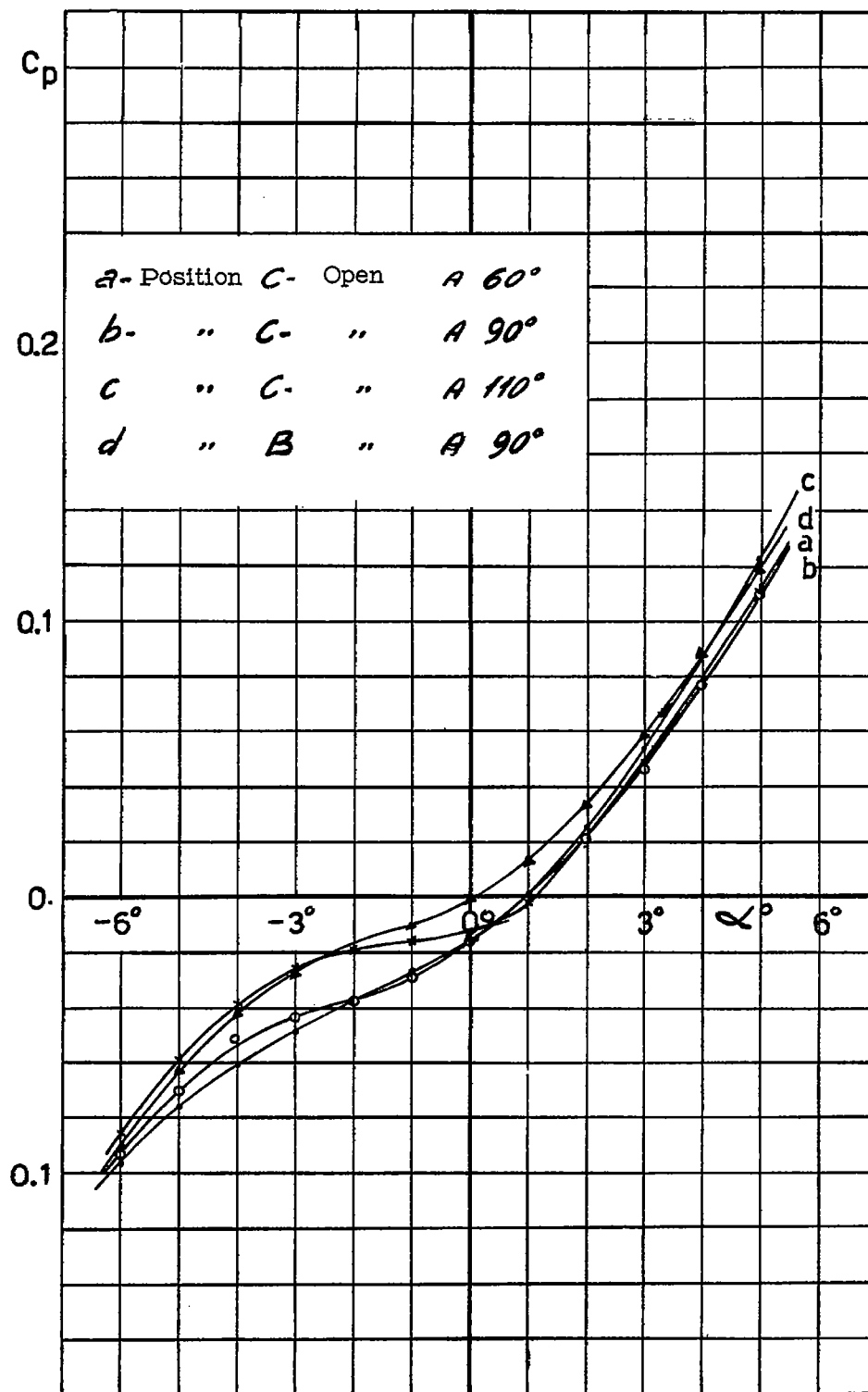
Figure 16.- Brake flaps, type 3 - perforations - lift.
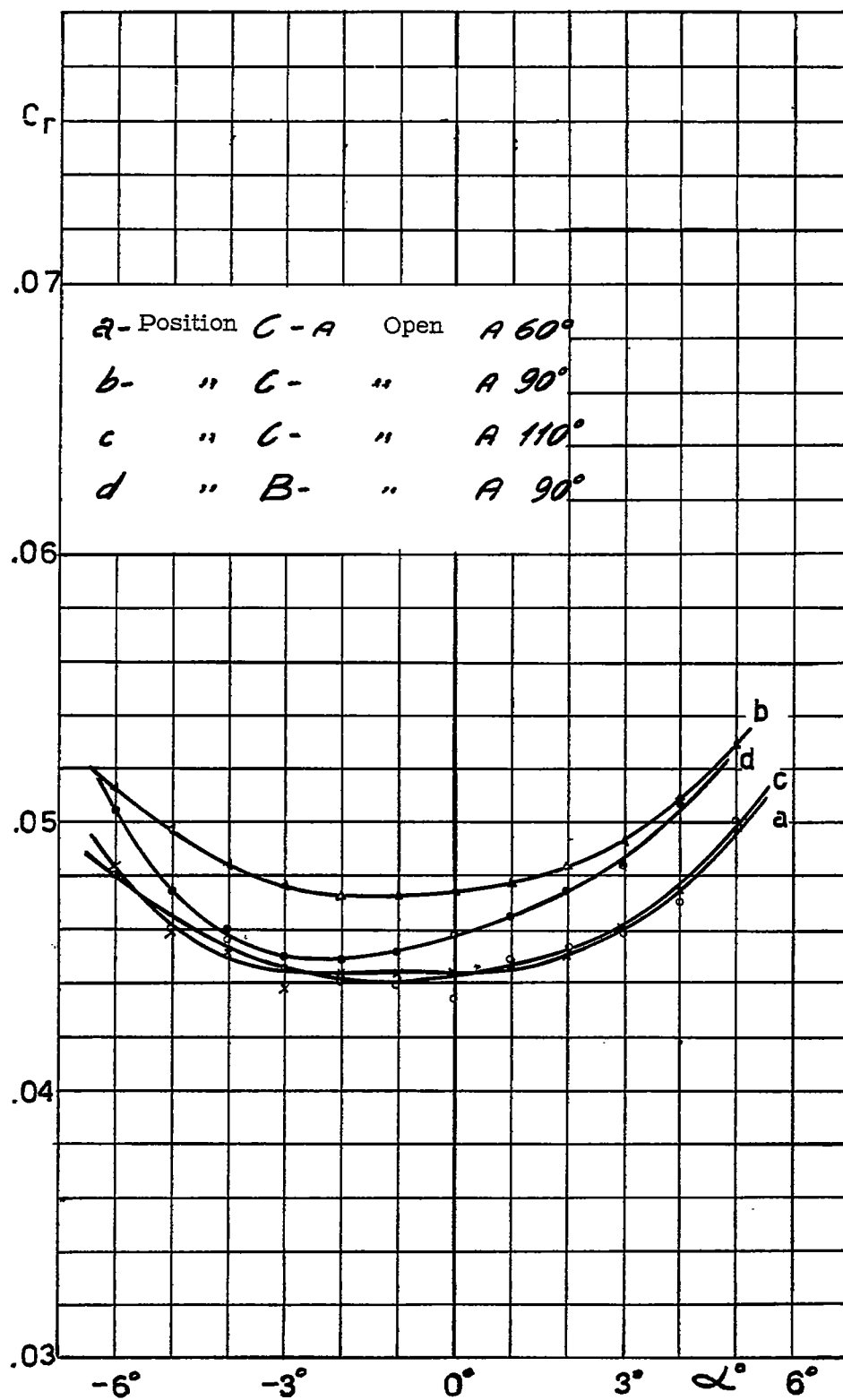
Figure 17.- Brake flaps, type 3 - perforations - drag.

C_p

a- Position C Open A $60°$
b-   " $C-$ " A $90°$
c-   " $C-$ " A $110°$
d   " $B-$ " A $90°$

0.2

0.1

0

-9   -6   -3   0   100 C_m 3

-0.1
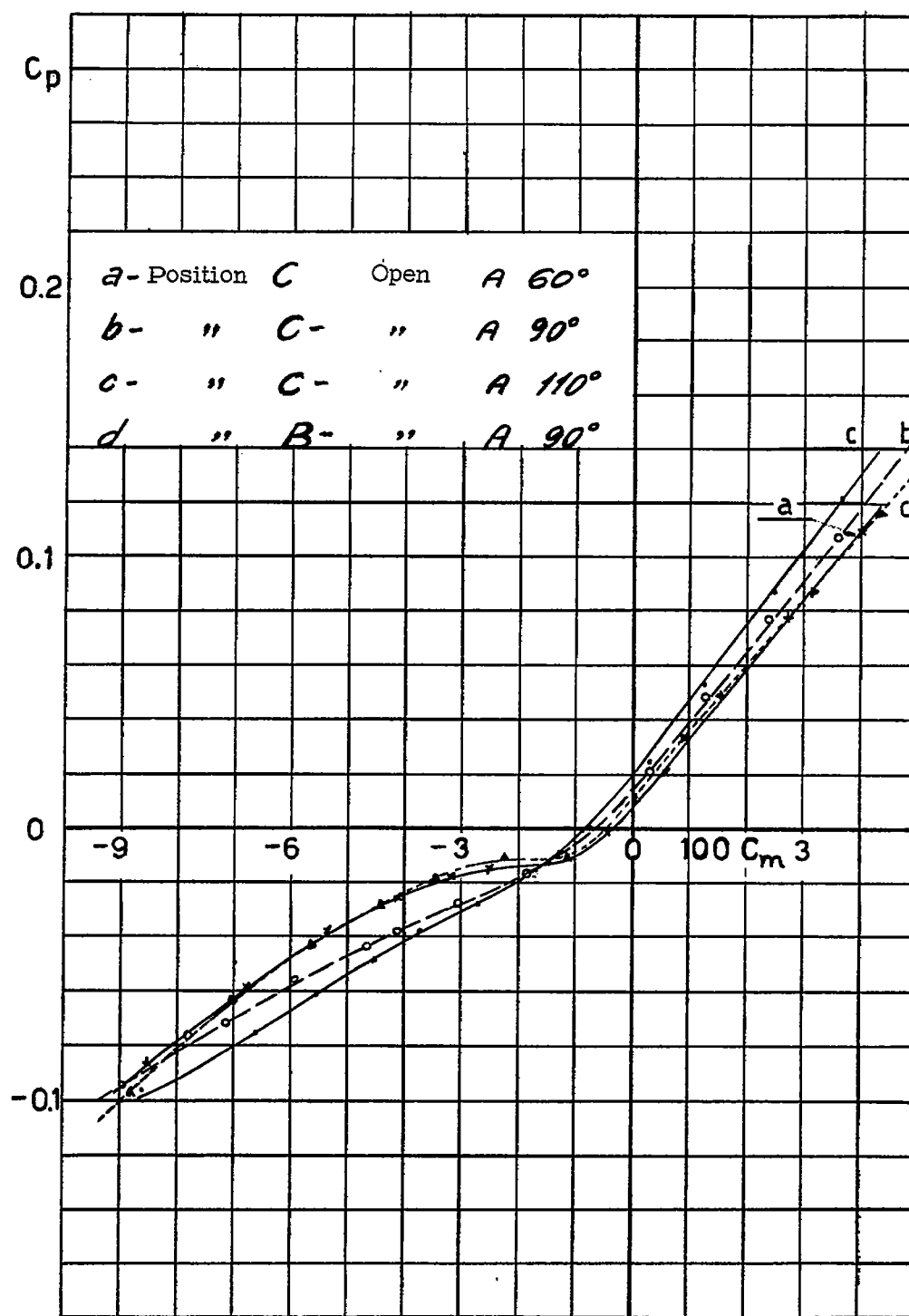
Figure 18.-   Brake flaps, type 3 - perforations - moments.
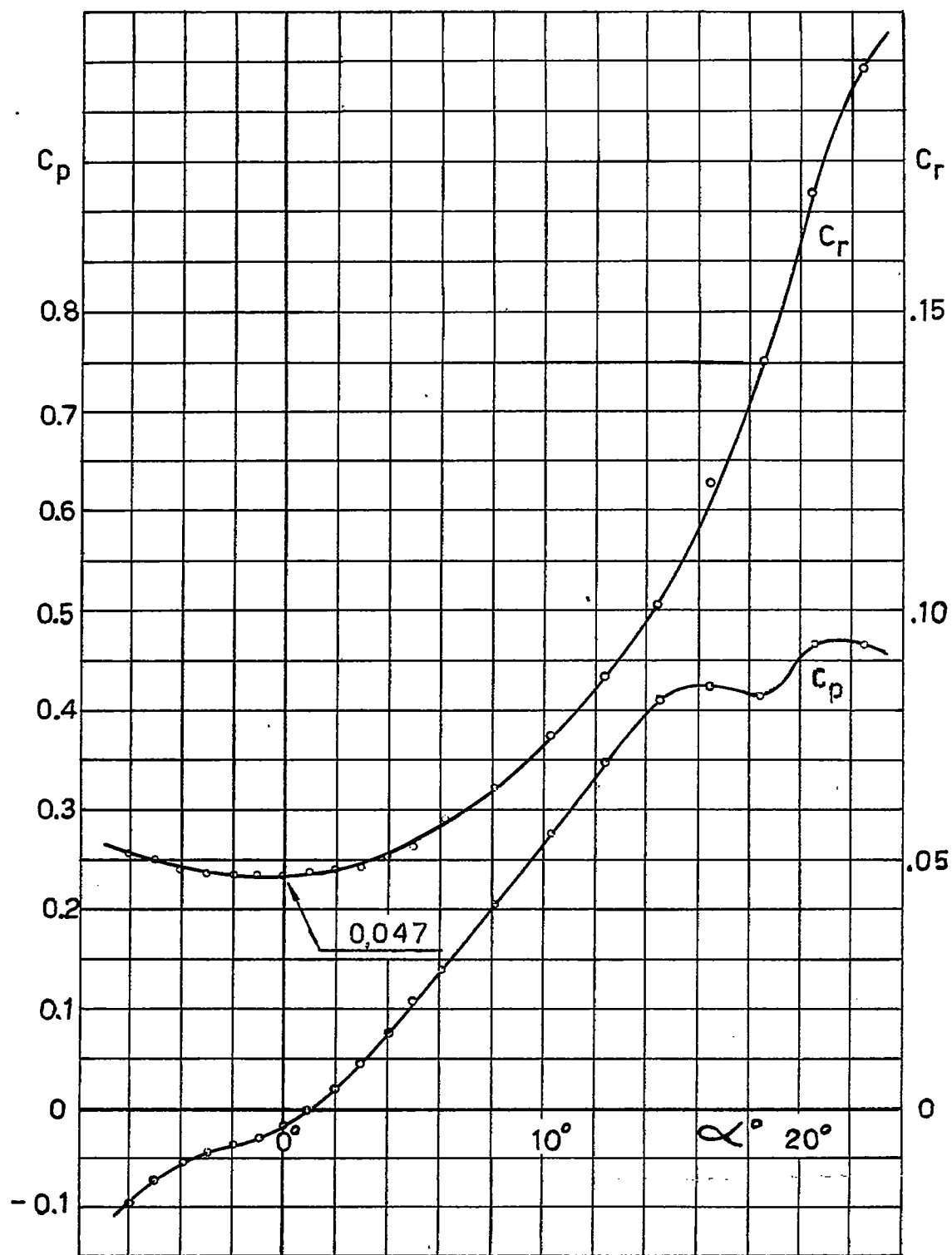
Figure 19.-   Brake flaps, type 3 - perforations, 90° open - position C -
lift and drag.
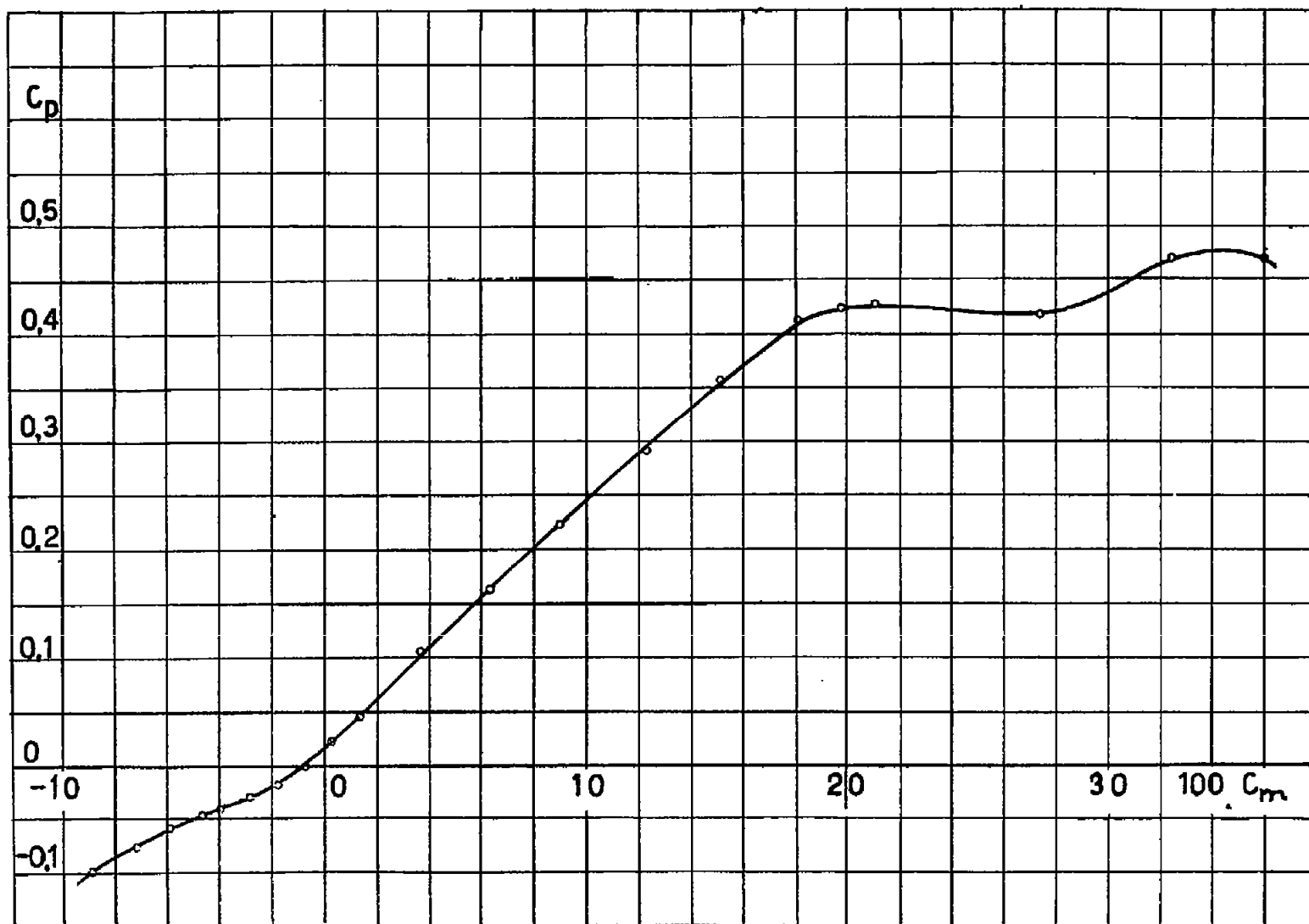
Figure 20.- Brake flaps, type 3 - perforations - 90° open - position C - moments.
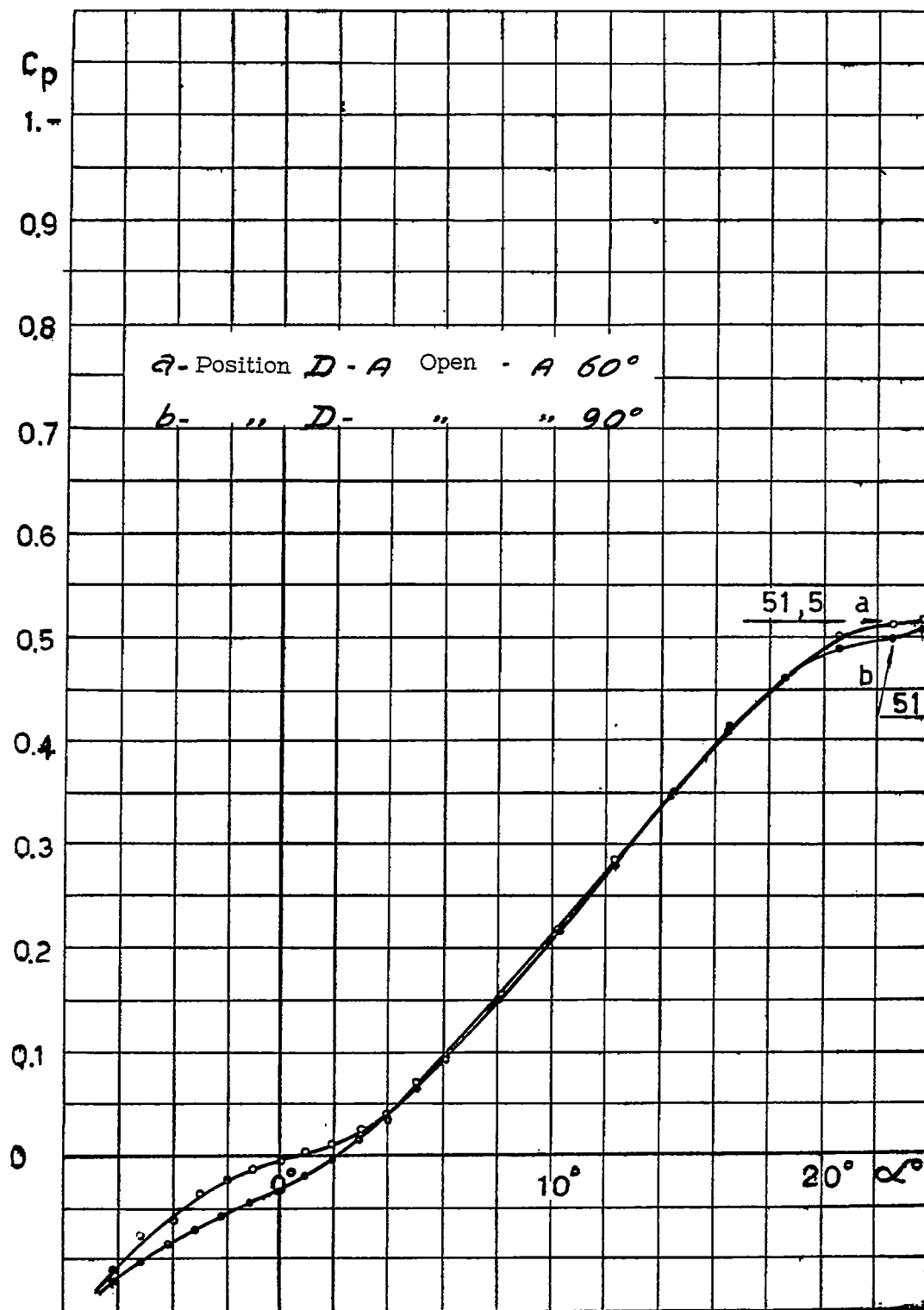
Figure 21.- Brake flaps, type 4 - lift.
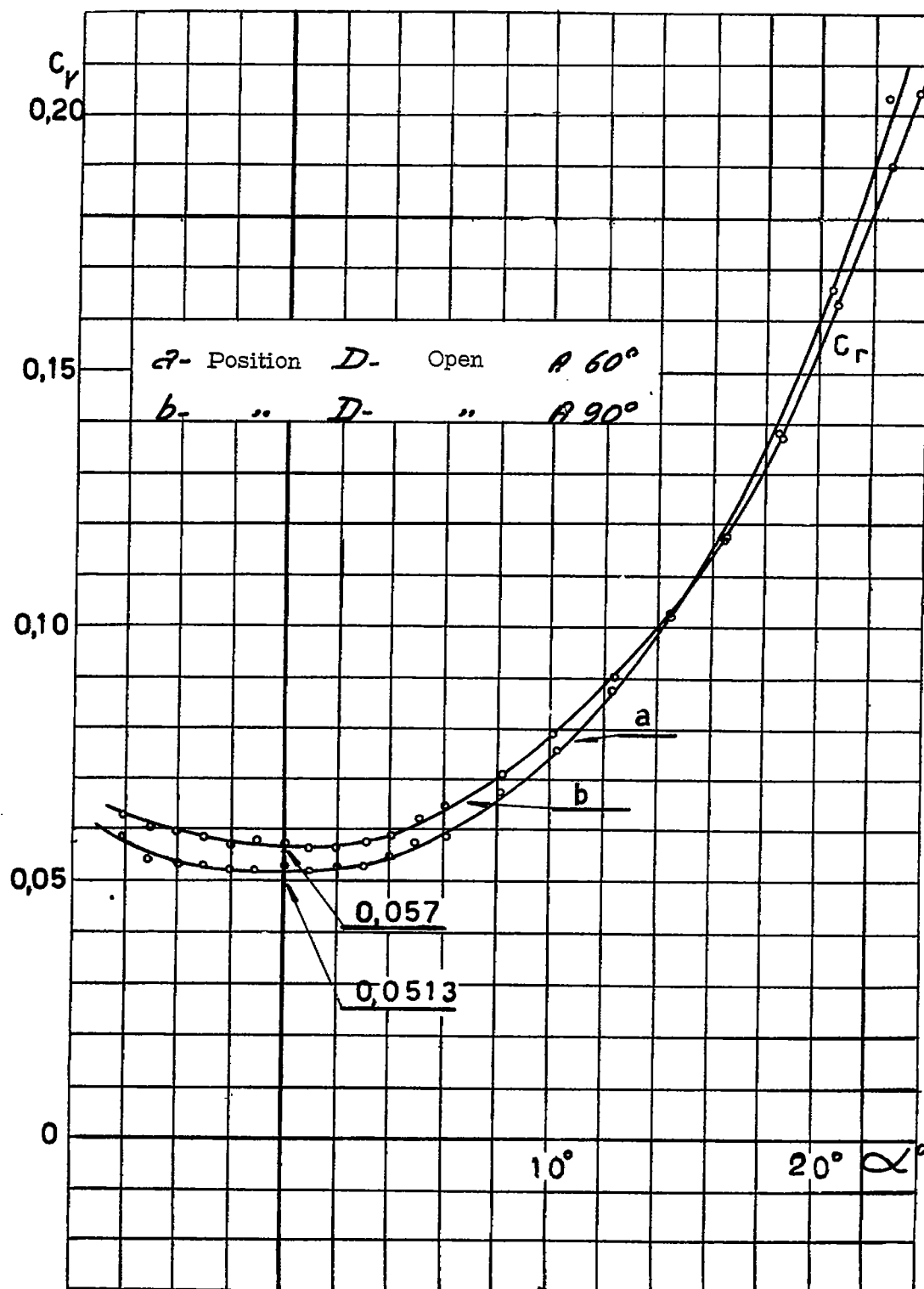
Figure 22.-   Brake flaps, type 4 - drag.
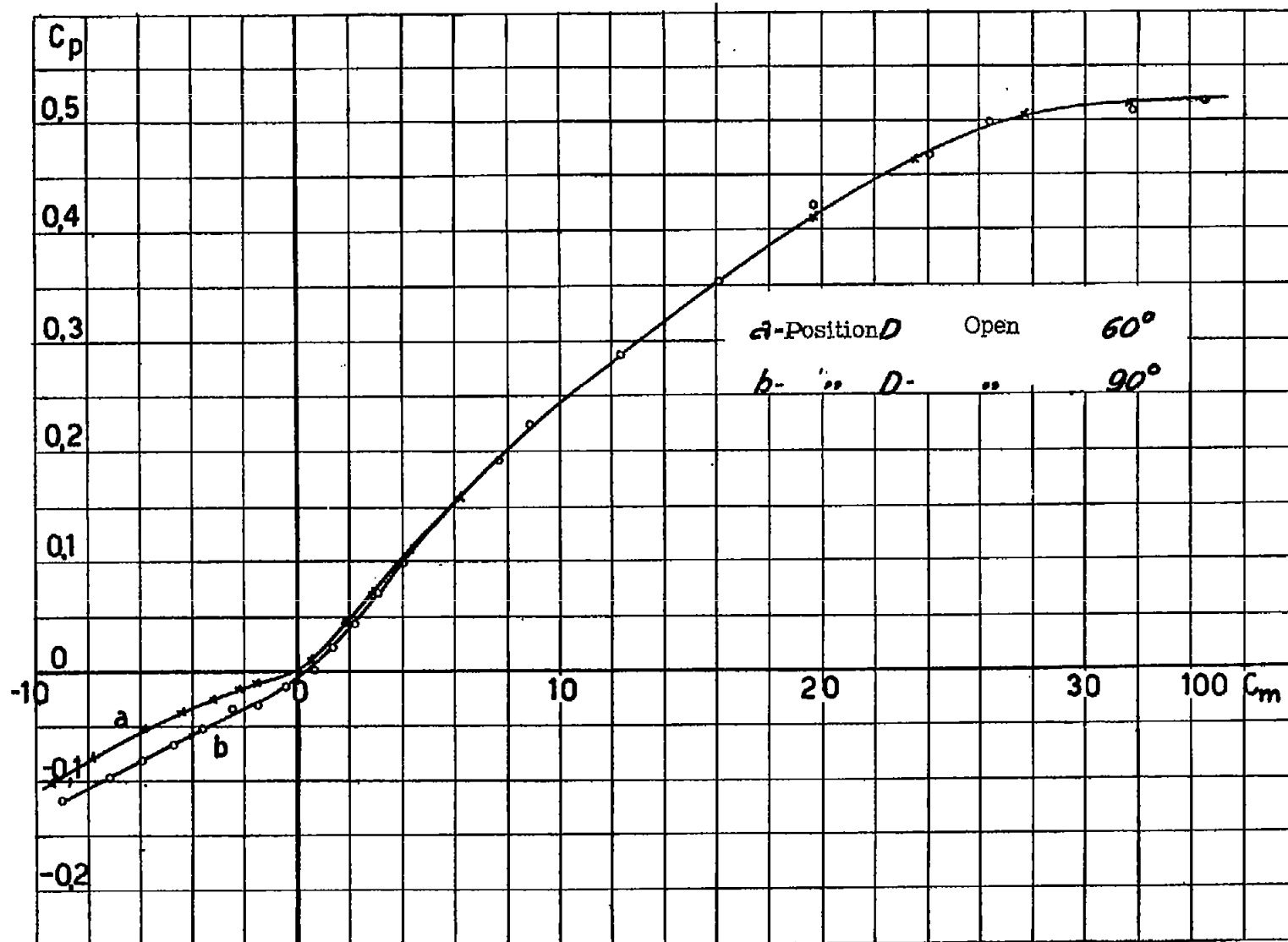
Figure 23.-   Brake flaps, type 4 - moments.

Figure 24.- Moments.

a - Type 3 perforations - position C - open 90°
b - Without brakes
c - Type 1 - position A
d - Type 1 - position A - flaps at 30°
e - Type 1 - position A - flaps at 60°
f - Type 4 - position D - open 60°
g - Type 4 - position D - open 90°
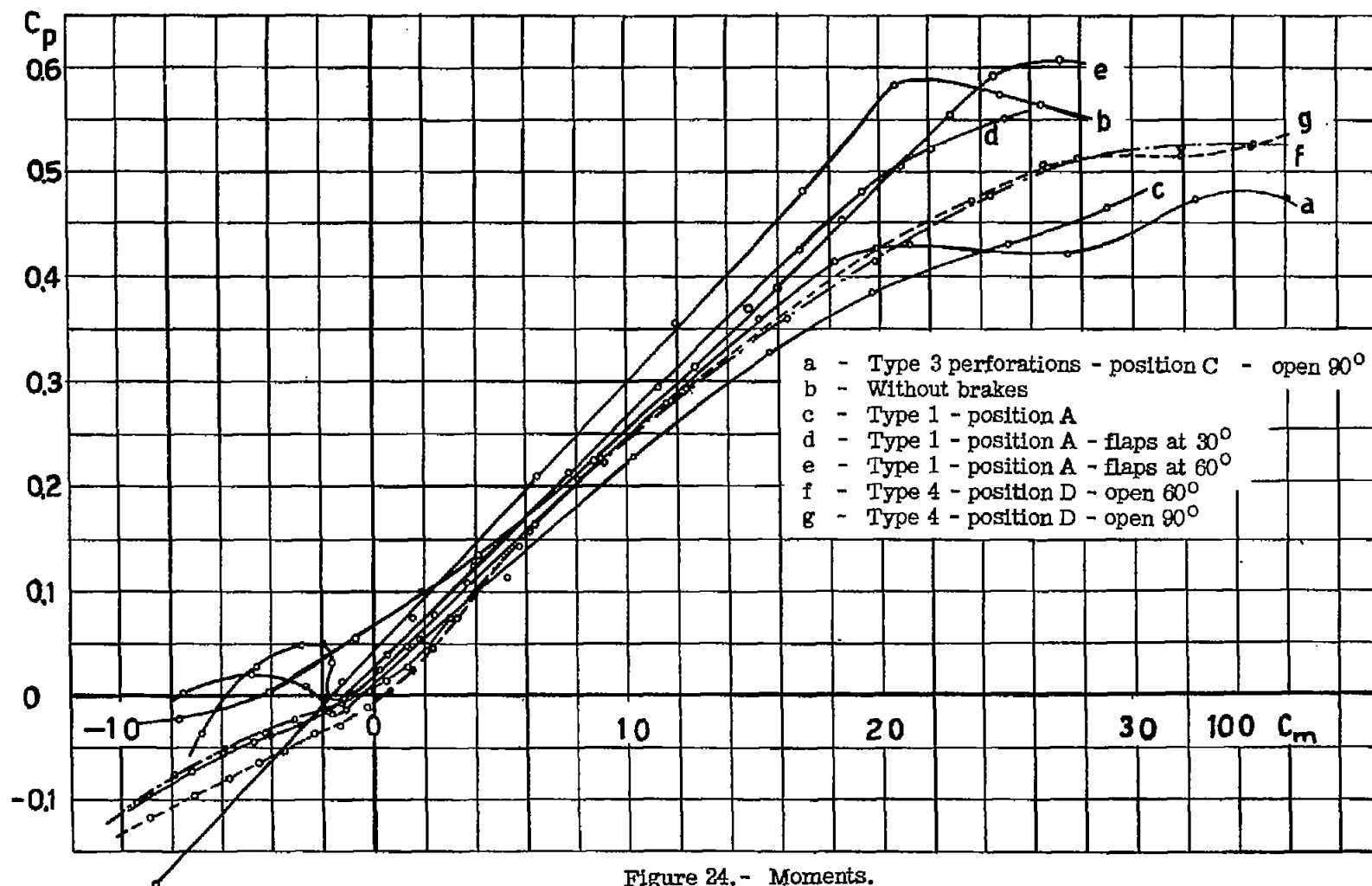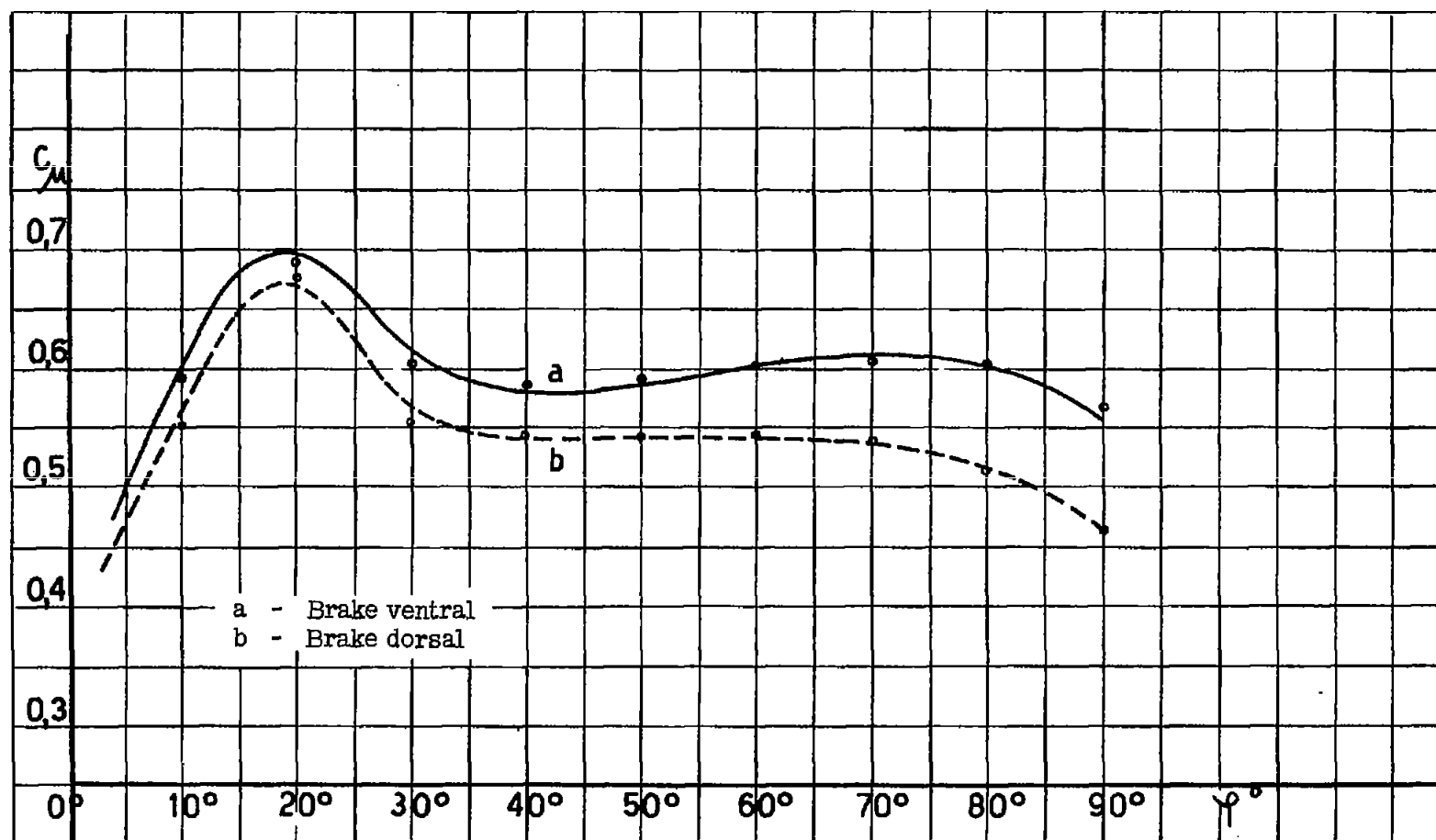
Figure 25.- Brake flaps, type 3 - hinge moments.
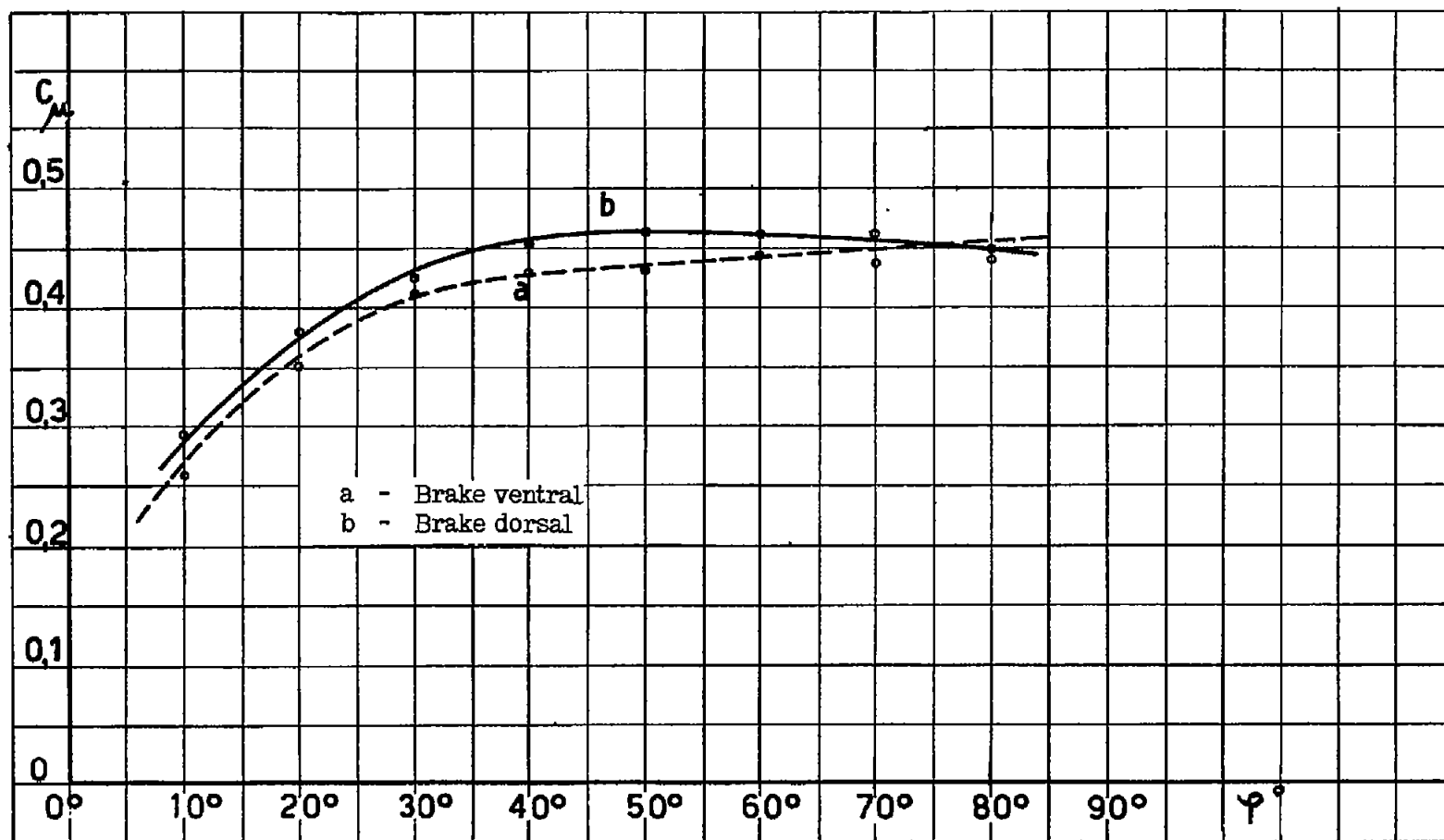
Figure 26.- Brake flaps, type 4 - hinge moments.
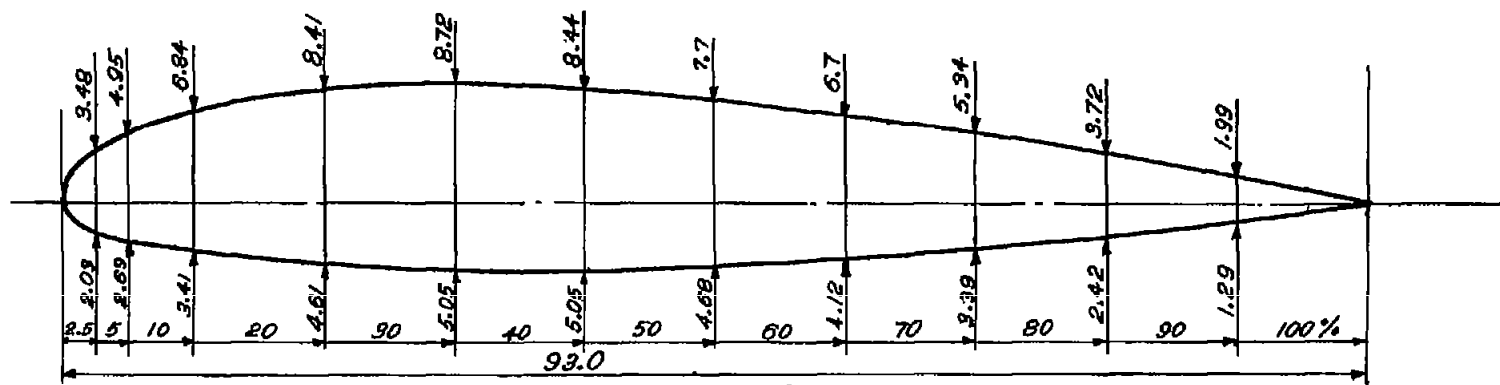
Airfoil   scale 1:5
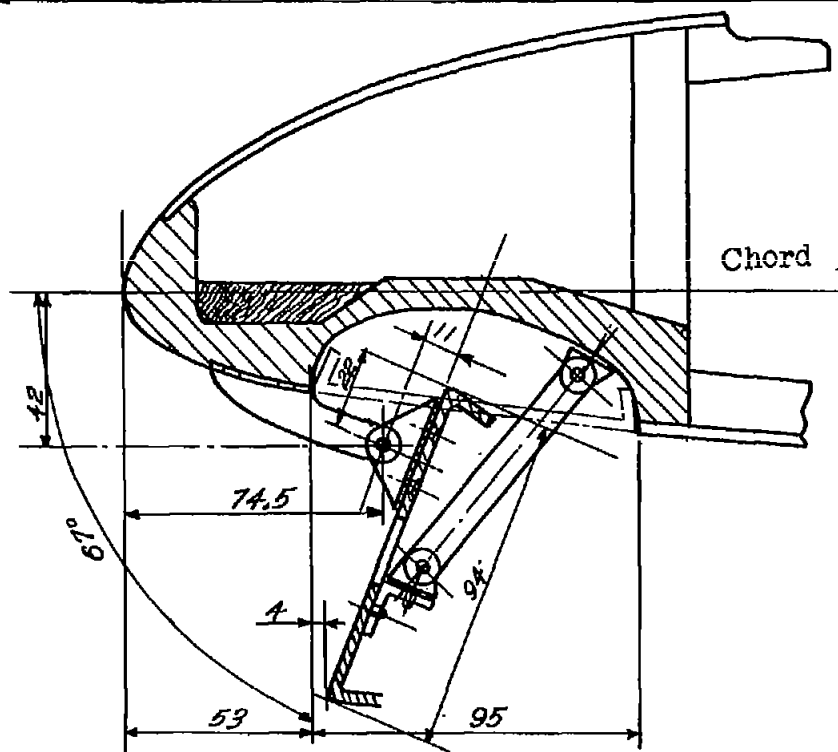
Plane of brake flap – scale 1:5

Chord
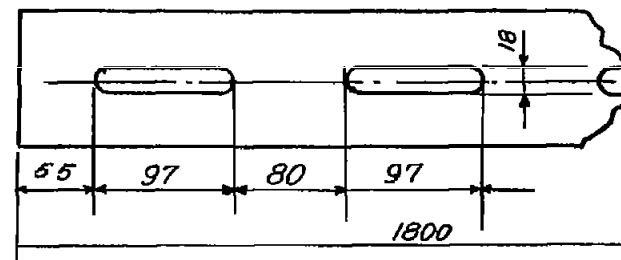
Details of ventral brake flap

Scale 1:2

Figure 27.- Details of upper-surface brake flap.
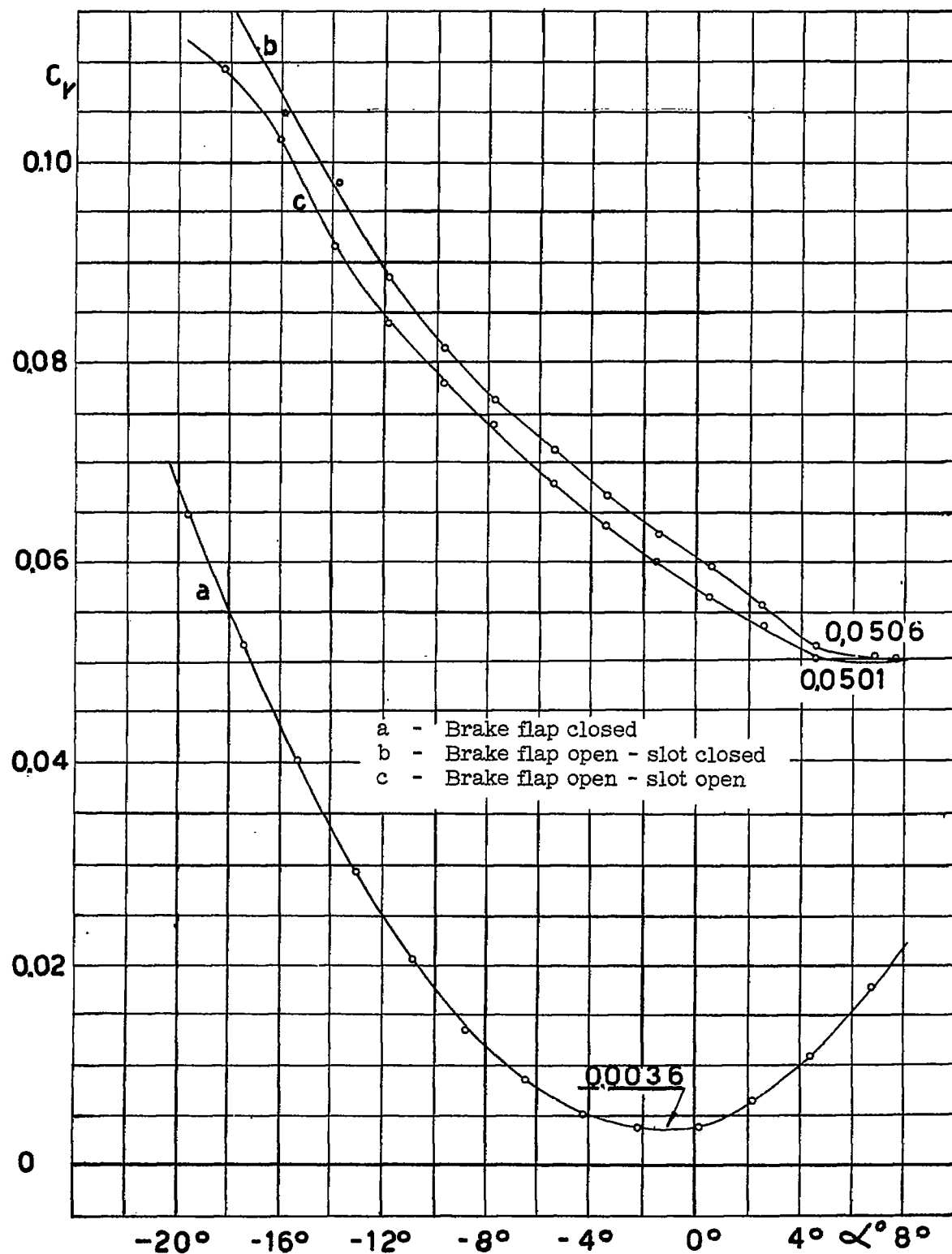
Figure 28.-   Ventral brake flap - drag.
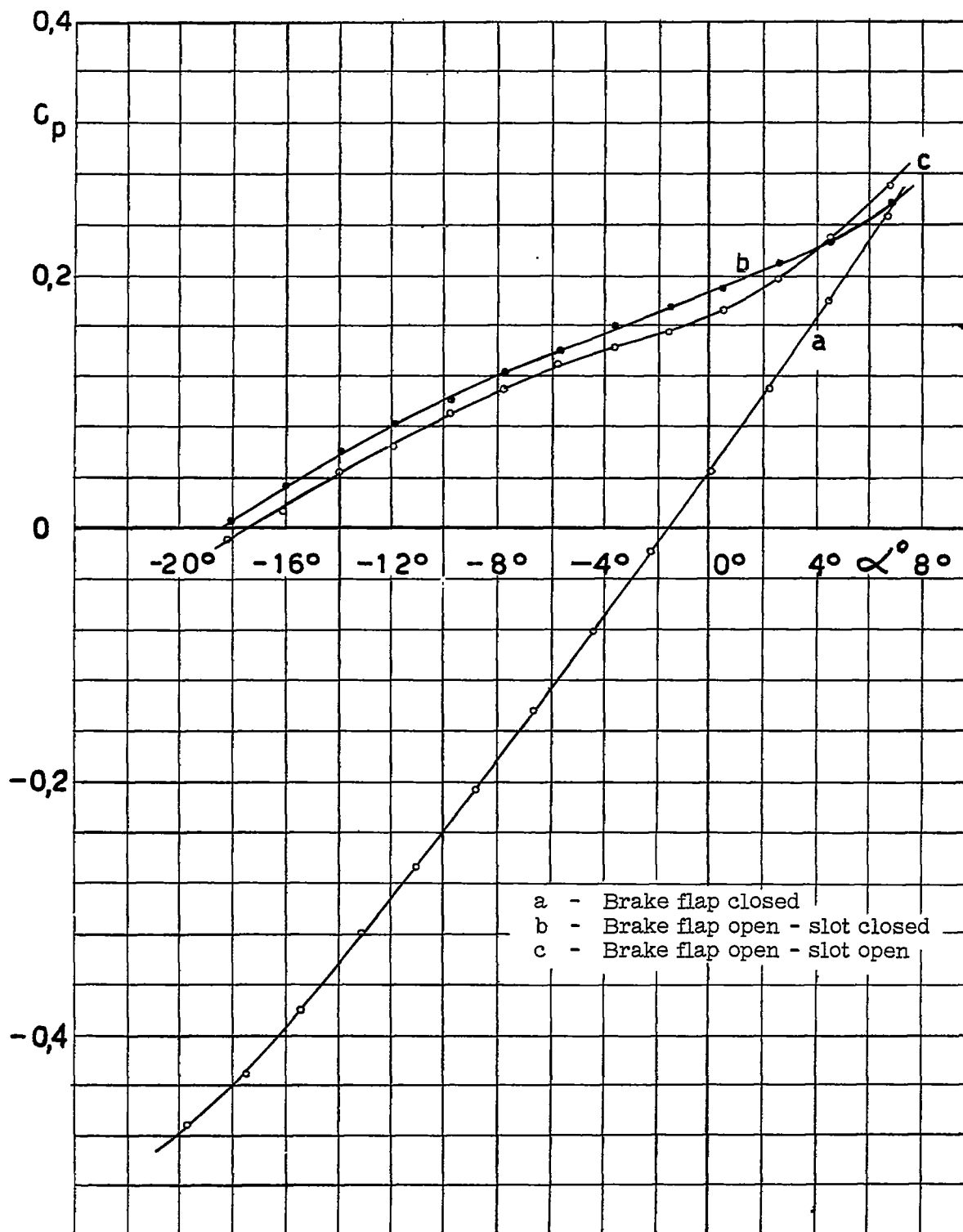
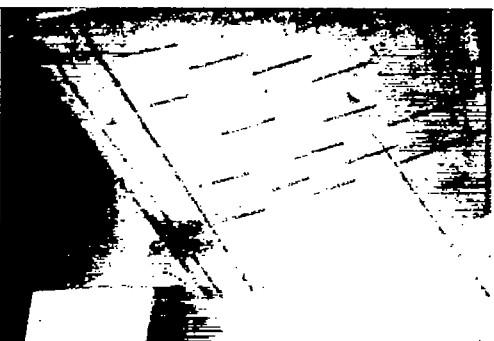Figure 29.- Ventral brake flap - lift.
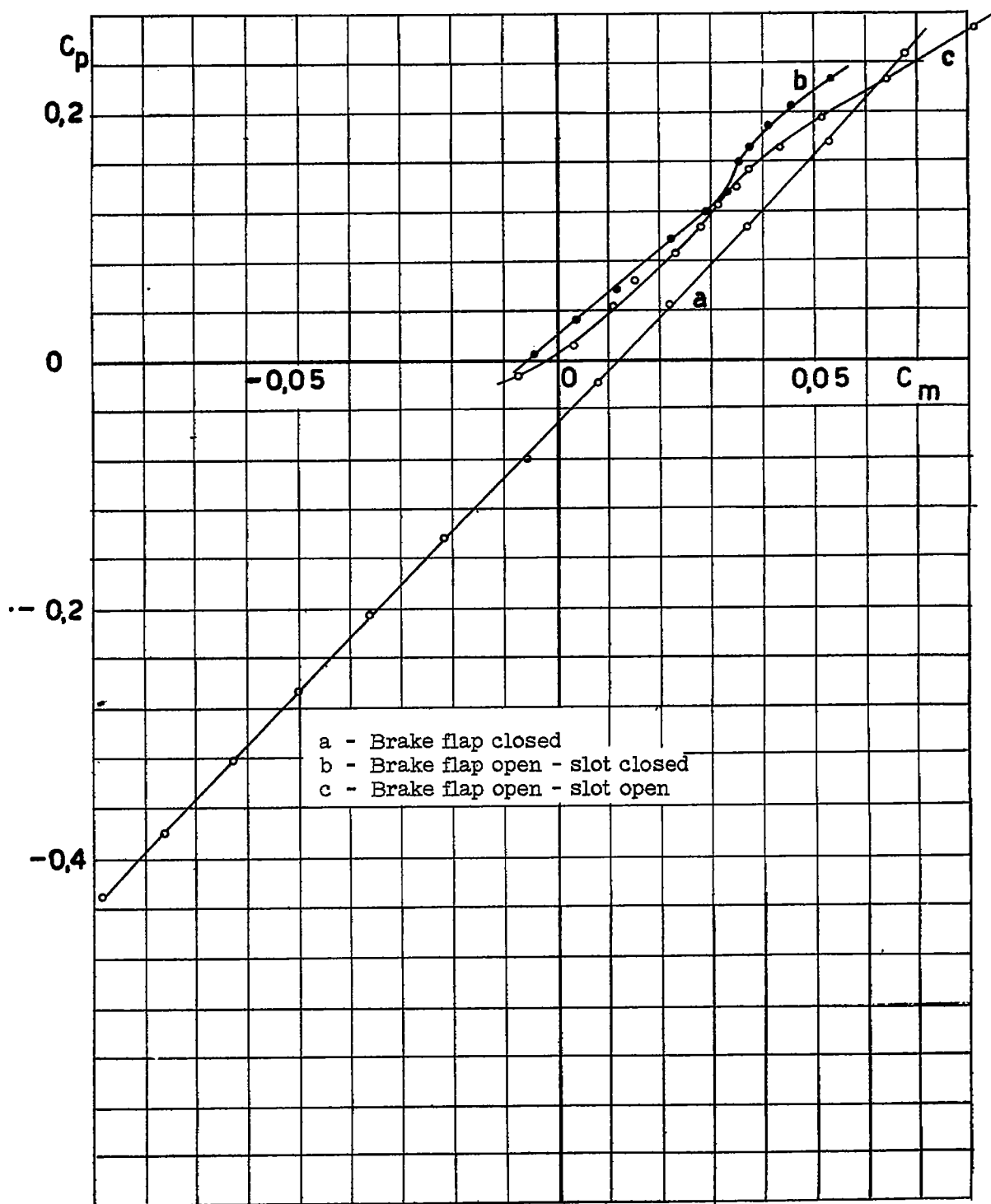
Figure 30.- Ventral brake flap - moments.
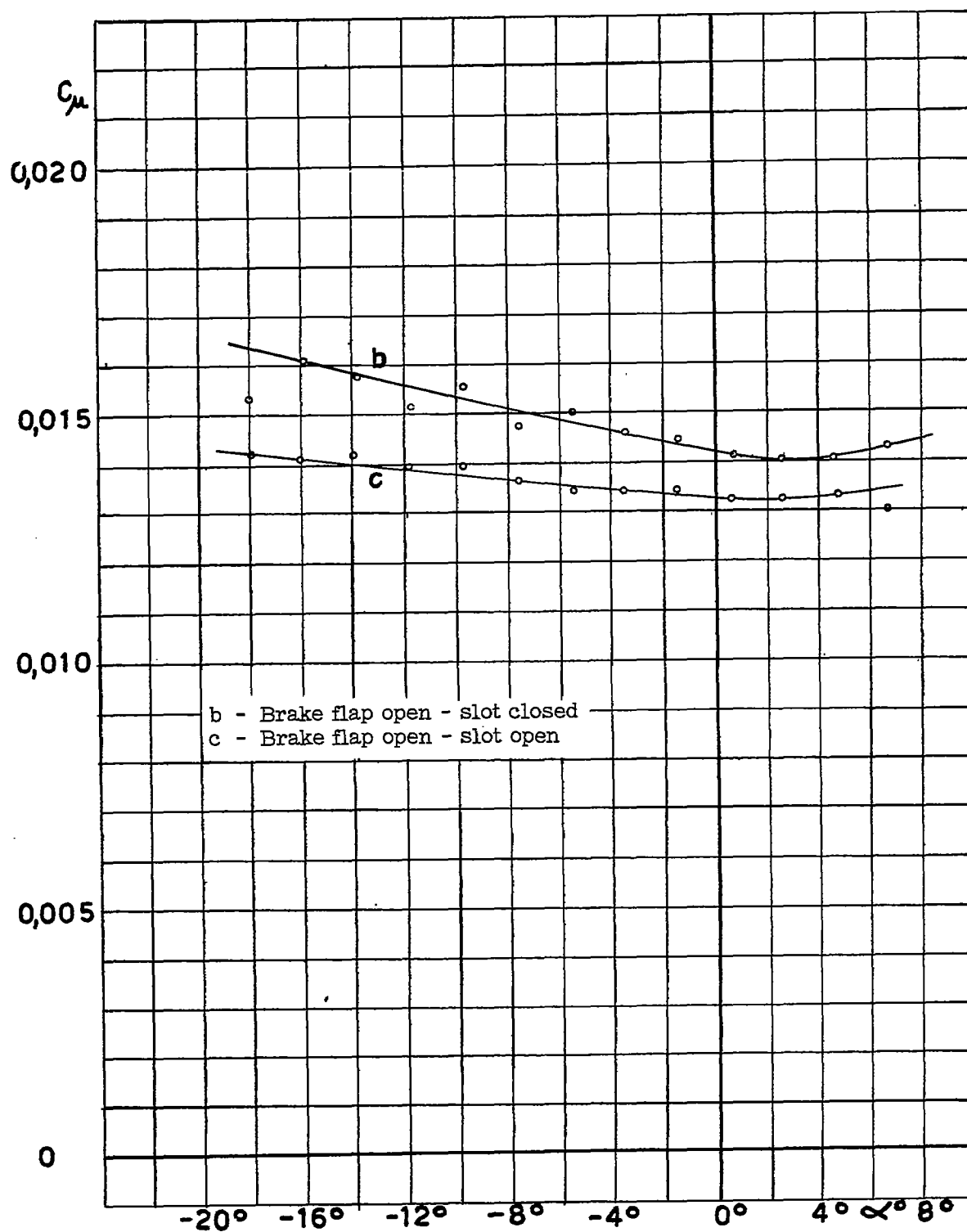
Figure 31.- Ventral brake flap - hinge moments.

b - Brake flap open - slot closed
c - Brake flap open - slot open
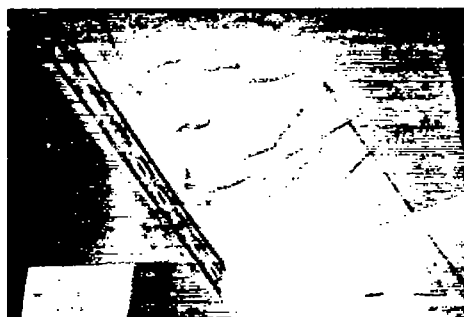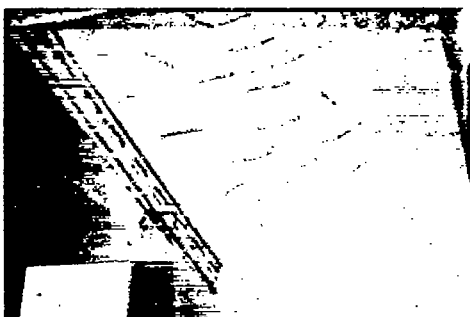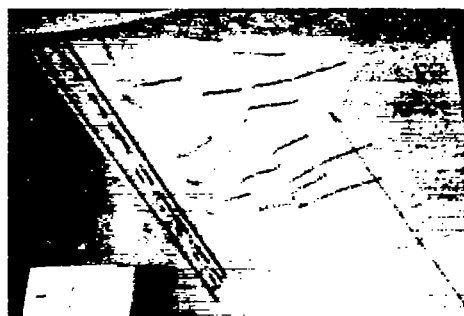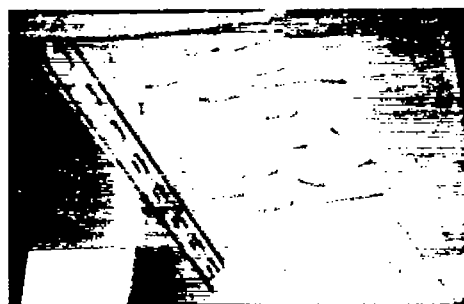
Brake flap open
Slots half open and half closed

Brake flap closed